Synthesis of interval-controlled polymers using monodisperse oligo(ethylene glycol)s by click chemistry and their functions

A Doctoral Thesis

by

Koki Ishitsuka

Submitted to

The Graduate School of Science, Osaka Universitty

February 2023

Acknowledgments

This thesis presents a research that the author has conducted at the Department of Macromolecular Science, Graduate School of Science, Osaka University, and supervised by Professor Akihito Hashidzume from 2017 to 2023.

Here the author expresses deep gratitude to Professor Akihito Hashidzume for his professional supervision. The author is also grateful for the large support of Associate Professor Yuri Kamon and Assistant Professor Masaki Nakahata.

This thesis was reviewed by Professors Akihito Hashidzume, Hiroyasu Yamaguchi, and Yoshinori Takashima. The author appreciates their careful review and helpful comments on this thesis.

The work on this thesis was partly financial-supported by JST SPRING, Grant Number JPMJSP2138.

Finally, the author would say many thanks to every single colleague, friend, and family who has stood in the author's life for their kindest support and warmest encouragement.

February 2023

石塚幸輝

Koki Ishitsuka

Department of Macromolecular Science

Graduate School of Science

Osaka University

Contents

Chapter 1

General Introduction

1-1. Challenge in Polymer Synthesis: Control of Intervals between Functional Groups

Biopolymers, e.g., proteins and nucleic acids, form higher-order structures based on strictly controlled monomer sequences to express various functions essential for biological activities.[1] In contrast, synthetic copolymers obtained through conventional polymerization techniques usually have distributions of monomer sequence and molecular weight. Since polymer properties are strongly dependent on the monomer sequence,[2,3] various strategies have been devised to synthesize sequence-controlled polymers.[4,5] Lutz et al.[6,7] reported synthesis of sequence-controlled polymers by controlled radical polymerization of electron-donating and accepting monomers. By adding a small amount of functional maleimides during atom transfer radical polymerization (ATRP) of styrene, various functionalities were introduced at arbitrary positions in the polymer chain. However, this technique has limitation to achieve complete control of monomer sequence. Satoh et. al.[8,9] synthesized sequence-regulated polymers by copper(I)-catalyzed radical addition of vinyl oligomers with olefin and

chlorine at the ends. The monomer sequence of the polymers was completely controlled, but the molecular weight was not controlled; the polymers exhibited a relatively broad molecular weight distribution. The solid-phase synthesis reported by Merrifield[10,11] is a technique that allows ones to synthesize specific monomer sequence and molecular weight. Protected amino acids are polymerized by repeated condensation and deprotection using beads as a solid phase to obtain oligopeptides with specific monomer sequence and molecular weight. Although solid phase synthesis is the most powerful tool for synthesis of polymers of specific monomer sequence and molecular weight (i.e., uniform polymers), it requires a long time and a lot of efforts.

In the design of synthetic polymers, it is necessary to control the interval of functional side chains to maximize the function of the polymers. Linking functional side chains to each other with a linker of a fixed length is a simple strategy to interval-controlled polymers. One of candidates for a system-independent universal linker is a monodisperse oligo(ethylene glycol) (MD-OEG).

1-2. Control of Group Intervals with Monodisperse Oligo(ethylene glycol)s as Linkers

The interval of functional side chains of polymers is an important parameter that

determines the polymer properties. For example, the mechanical properties of network polymers depend on the interval between cross-linking points. As the interval between cross-linking points decreases, the density of cross-linking points increases, resulting in an increase in Young's modulus. However, network polymers of a high cross-linking density are usually fragile presumably because of heterogenous distribution of cross-linking points. This is because the stress is concentrated in dense cross-liking regions. Sakai et al.[12,13] synthesized uniform network polymers using tetra-armed poly(ethylene glycol)s (PEGs) with narrow molecular weight distribution. The obtained polymers exhibited excellent mechanical properties based on the uniform network structure (Figure 1-1).

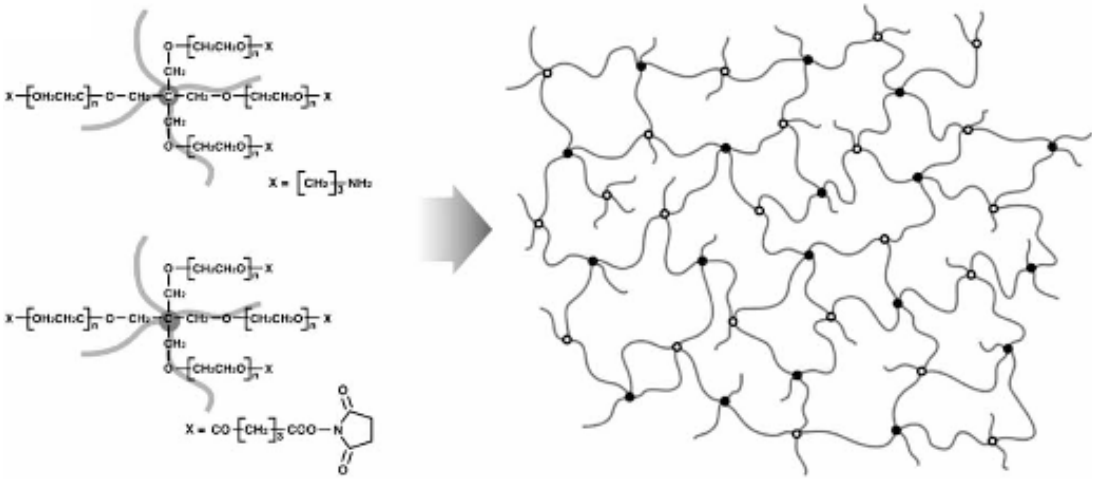

Figure 1-1. Illustration of the gel formed from tetra-armed poly(ethylene glycol)s. Reprinted with permission from ref. 13. Copyright 2010 WILEY-VCH.

The aggregation behavior of polymers is influenced by intervals between the main chain and functionalities in side chains. Farhangi and Duhamel[14] prepared methacrylate monomers bearing a pyrenyl (Py) group linked through monodisperse oligo(ethylene glycol) (MD-OEG) linkers of different molecular weights, and copolymerized the Py-carrying methacrylates with butyl methacrylate. They investigated the effect of the length of MD-OEG spacer on photophysical properties of the Py-labeled polymers by steady-state and time-resolved fluorescence measurements. They have demonstrated that Py excimers form more favorably for a polymer of a longer MD-OEG spacer. This is because the flexible longer MD-OEG spacer increases the encounter probability of excited and ground state Py moieties (Figure 1-2).

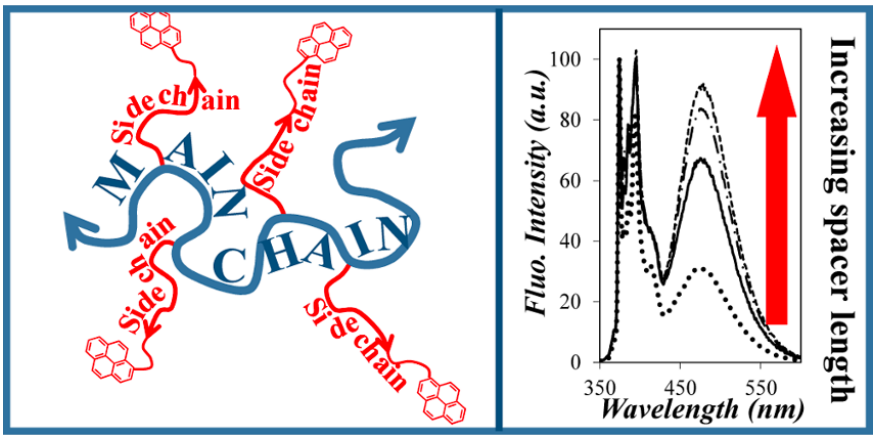

Figure 1-2. The effect of the length of MD-OEG spacer on photophysical properties of the pyrene-labeled polymers. Reprinted (adapted) with permission from ref. 14. Copyright 2016 American Chemical Society.

The interval between functional groups that interact with each other is a key for the formation of supramolecular complexes. Maartje et al.[15] synthesized ditopic compounds possessing S-protein and S-peptide, a pair that form a supramolecular complex (ribonuclease S) by strong noncovalent interaction (association constant $K_a \sim 7 \times 10^6$ M^{-1} in aqueous sodium acetate at 25 °C), using MD-OEG linkers of different lengths. They analyzed the complexes by a combination of size exclusion chromatography (SEC) and mass spectrometry (MS). Cyclic oligomers with different degrees of polymerization were formed depending on the length of MD-OEG and the concentration of the ditopic compound (Figure 1-3).

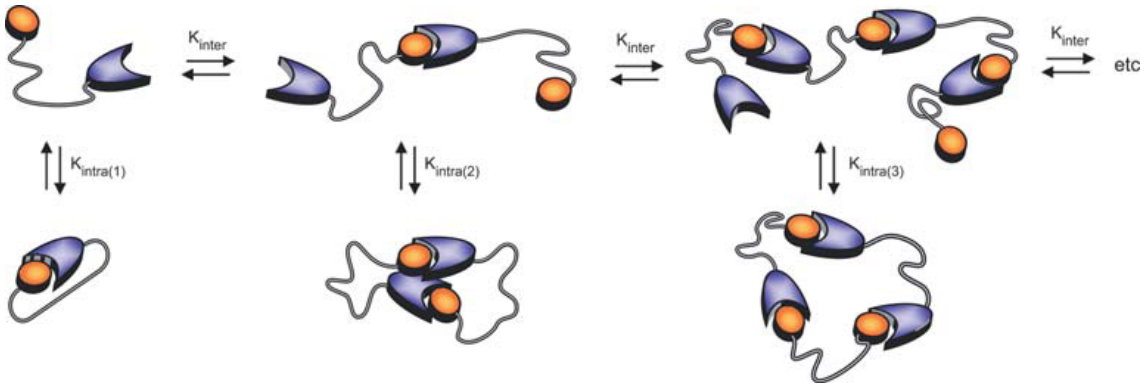

Figure 1-3. Schematic illustration of the ring–chain supramolecular polymerization of the ditopic compound. Repritend with permission from ref. 15. Copyright 2010 Royal Society of Chemistry.

These studies have demonstrated that the polymer function strongly depends on the interval of functional groups and MD-OEG is useful to synthesis of interval-controlled polymers or oligomers. Thus, the author focuses on MD-OEG as a spacer to synthesize polymers or oligomers with controlled intervals of functional groups in this study.

1-3. Click Chemistry for Synthesis of Various Polymers and Oligomers

Click chemistry, proposed by Kolb et al.[16] in 2001, is a technique to create new functional molecules from simple molecules using several robust reactions. The reactions used in click chemistry, so-called click reactions, include copper(I)-catalyzed azide–alkyne cycloaddition (CuAAC),[17–19] thiol–ene reaction,[20–22] thiol–yne reaction,[23,24] Diels–Alder reaction,[25,26] nitrile *N*-oxide–ene reaction,[27,28] and nucleophilic ring opening reactions of three-membered heterocycles.[29] CuAAC is a reaction catalyzed by copper(I) compounds to form 1,4-disubstituted 1,2,3-triazole from azide and alkyne groups under mild conditions (Scheme 1-1A).[19] When strained alkynes are used, the reaction proceeds efficiently without any catalysts (strain-Promoted azide–alkyne cycloaddition, SPAAC).[30,31] Thiol–ene reaction is addition of thiol to alkene in radical or anionic mechanism to form thioether (Scheme 1-1B).[21] When alkynes are used instead of alkenes (i.e., thiol–yne reaction), two equivalents of thiol react with one equivalent of alkyne to

form dithioether (Scheme 1-1C).[23,24] Diels-Alder reaction forms cyclohexene structure from conjugated diene and alkene (Scheme 1-1D).[25] Extremely electron-deficient heterocycles such as tetrazine and triazine react rapidly with strained alkenes at room temperature (strain-promoted inverse electron-demand Diels–Alder Cycloaddition, SPIEDAC).[32] Nitrile *N*-oxide–ene reaction is cycloaddition of nitrile *N*-oxide to alkene to form isoxazoline ring (Scheme 1-1E).[27] Three-membered heterocycles including epoxide and aziridine readily undergo a nucleophilic ring-opening reaction (Scheme 1-1F).[29] These reactions proceed efficiently and selectively even in the presence of many types of functional groups. Therefore, click chemistry has been used for the synthesis of various polymers including network polymers,[33–35] branched polymers,[36–38] and cyclic polymers.[39–41] In addition, taking advantage of the selectivity and efficiency, uniform oligomers have been synthesized by stepwise click reactions.[42–45]

Based on the above, the author hypothesizes that a combination of MD-OEG and click chemistry is a powerful method for synthesis of interval-controlled polymers carrying functional groups.

Scheme 1-1. CuAAC (A), Thiol–Ene Reaction (B), Thiol–Yne Reaction (C), Diels–Alder Reaction (D), Nitrile *N*-Oxide–Ene reaction (E), Nucleophilic Ring-Opening Reactions of Three-Membered Heterocycles (F)

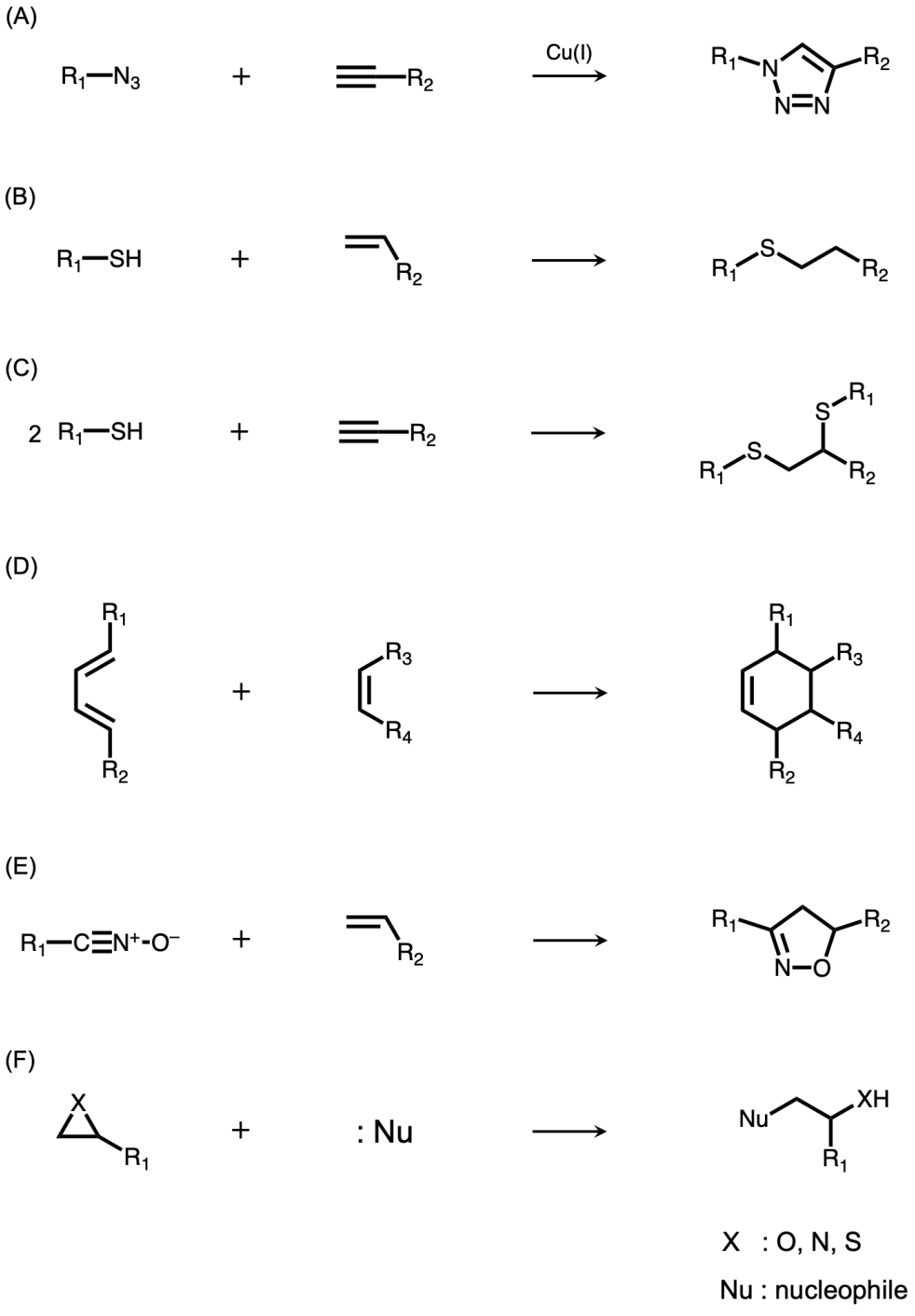

1-4. Scope of This Thesis

In this thesis, therefore, the author reports the synthesis of interval-controlled polymers and oligomers using a combination of MD-OEG and click chemistry and their functions based on the controlled intervals of functional groups.

In Chapter 2, the author focuses on the thiol–yne reaction to prepare homogeneous network polymers. Network polymers are synthesized by the thiol–yne reaction using MD-OEGs of different molecular weights carrying thiol and alkyne moieties, respectively at both the ends. Mechanical properties of the polymers are characterized by compression tests. Young's modulus of the network polymers decreased with increasing *n*, which is the degree of polymerization of MD-OEG, because of the decrease in crosslink density (Figure 1-4).

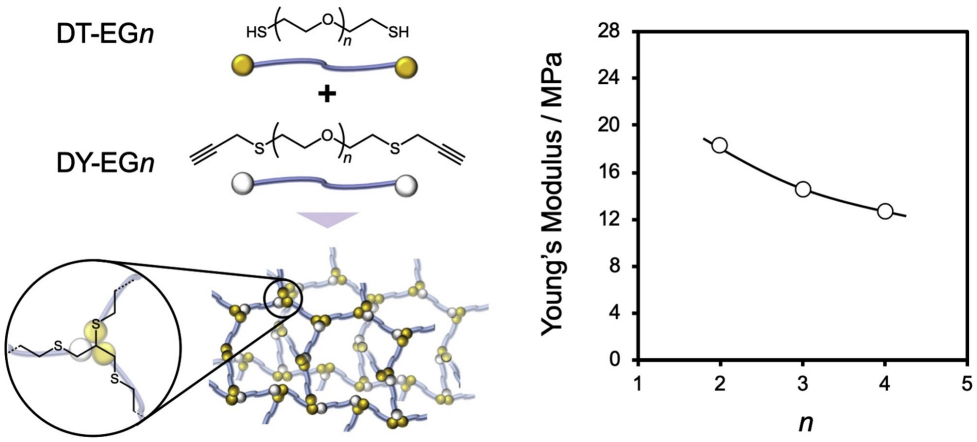

Figure 1-4. Typical illustration of the polymer network formed from MD-OEGs of different molecular weights and their mechanical properties.

In Chapters 3 and 4, the author reports on the synthesis of interval-controlled cyclic dimers and their interactions aiming at detailed studies on interactions of multivalent molecules.

In Chapter 3, the author synthesizes a uniform cyclic dimer (*c*-ene2) by stepwise CuAAC of a diazide formed from triethylene glycol and a dialkyne possessing an internal alkene. Cyclic dimers bearing adamantyl (Ad) and β-cyclodextrin (βCD) moieties are synthesized by thiol–ene reaction of *c*-ene2.

In Chapter 4, the author investigates the interactions of the cyclic dimers synthesized in Chapter 3. Firstly, the interactions of cyclic host dimer bearing βCD moieties (*c*-βCD2) with polyacrylic acid p(AANa/Np*x*) bearing naphthyl (Np) residues of different contents are investigated by fluorescence measurements. The interactions of p(AANa/Np*x*) with βCD are analyzed by a one-to-one complex formation model. On the other hand, the interactions of p(AANa/Np*x*) are analyzed by a model for the formation of higher-order complexes, i.e., two-to-two complexes. The first association constant (K_1) for the two-to-one complex formation is larger than the second association constant (K_2) for the two-to-two complex formation, indicative of negative cooperativity presumably because of the mismatched intervals of Np and βCD moieties. The interactions of cyclic dimer bearing Ad moieties (*c*-Ad2) with βCD, βCD dimers linked by disulfide bonds

(βCD2-1 and βCD2-2), and the cyclic host dimer (*c*-βCD2) are investigated by ^{1}H NMR. The interactions of *c*-Ad2 with βCD and βCD2-1 are explained by a one-to-one complex formation model. On the other hand, the interactions of *c*-Ad2 with βCD2-2 and with *c*-βCD2 were explained by the Hill model with $n \sim 2$, indicative of positive cooperativity presumably because of the matched intervals of Ad and βCD moieties (Figure 1-5).

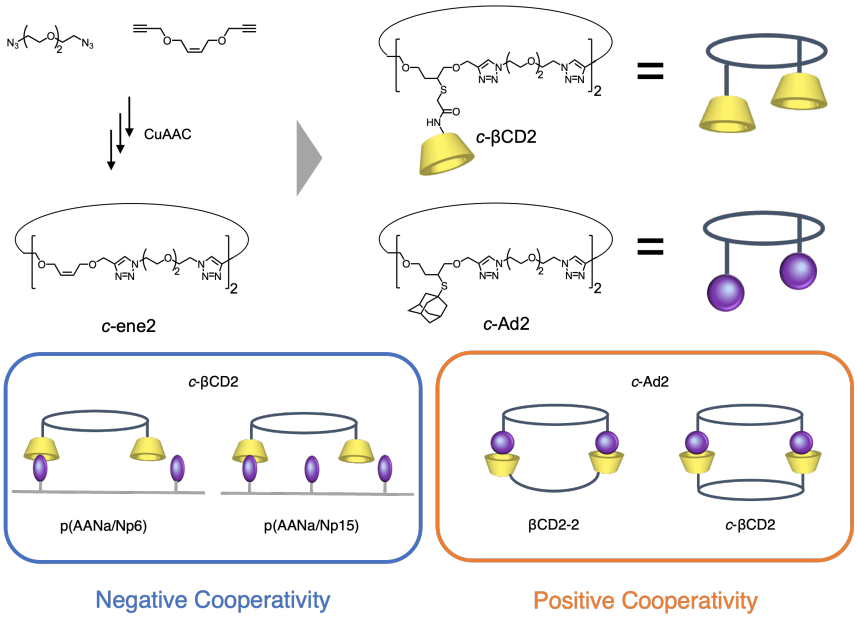

Figure 1-5. Conceptual illustration of negative cooperative interaction of p(AANa/Np6) and p(AANa/Np15) with *c*-βCD2 and positive cooperative interaction of *c*-Ad2 with βCD2-2 and *c*-βCD2.

Chapter 5 summarizes the main findings and conclusions from this thesis.

1-5. References

(1) Voet, D.; Voet, J. G. *Biochemistry*; 4th ed.; Wiley & Sons: New York, 2010.

(2) Zheng, Y.; Cai, S.; Peng, Li.; Jin, Y.; Xu, H.; Weng, Z.; Gao, Z.; Zhao, B.; Gao, C. *Polym. Chem.* **2016**, *7*, 6202–6210.

(3) Kametani, Y.; Sawamoto, M.; Ouchi, M. *Angew. Chem. Int. Ed.* **2018**, *57*, 10905–10909.

(4) Lutz, J.-F.; Ouchi, M.; Liu, D. R.; Sawamoto, M. *Science* **2013**, 341, 1238149.

(5) Lutz, J.-F. *Macromol. Rapid Commun.* **2017**, *38*, 1700582.

(6) Pfeifer, S.; Lutz, J.-F. *J. Am. Chem. Soc.* **2007**, *129*, 9542–9543.

(7) Lutz J.-F.; Schmidt B. V. K. J.; Pfeifer S. *Macromol. Rapid Commun.* **2011**, *32*, 127–135.

(8) Satoh K.; Mizutani M.; Kamigaito M. *Chem. Commun.* **2007**, *12*, 1260–1262.

(9) Satoh K.; Ozawa S.; Mizutani M.; Nagai K.; Kamigaito M. *Nat. Commun.* **2010**, *1*, 6.

(10) Merrifield R. B. *J. Am. Chem. Soc.* **1963**, *85*, 2149–2154.

(11) Merrifield R. B. *Science* **1986**, *232*, 341–347.

(12) Sakai, T.; Matsunaga, T.; Yamamoto, Y.; Ito, C.; Yoshida, R.; Suzuki, S.; Sasaki, N.; Shibayama, M.; Chung, U.-i. *Macromolecules* **2008**, *41*, 5379–5384.

(13) Sakai, T.; Akagi, Y.; Matsunaga, T.; Kurakazu, M.; Chung, U.-i.; Shibayama, M. *Macromol. Rapid Commun.* **2010**, *31*, 1954–1959.

(14) Farhangi, S.; Duhamel, J. *Macromolecules* **2016**, *49*, 353−361.

(15) Maartje, M. C. Bastings, M. M. C.; de Greef, T. F. A.; van Dongen, J. L. J.; Merkx, M.; Meijer, E. W. *Chem. Sci.* **2010**, *1*, 79–88.

(16) Kolb, H. C.; Finn, M. G.; Sharpless, K. B. *Angew. Chem. Int. Ed.* **2001**, *40*, 2004–2021.

(17) Rostovtsev, V. V.; Green, L. G.; Fokin, V. V.; Sharpless, K. B. *Angew. Chem., Int. Ed.* **2002**, *41*, 2596–2599.

(18) Tornøe, C. W.; Christensen, C.; Meldal, M. *J. Org. Chem.* **2002**, *67*, 3057–3064.

(19) Worell, B. T.; Malik, J. A.; Fokin, V. V. *Science* **2013**, *340*, 457–460.

(20) Posner, T. *Chem. Ber.* **1905**, *38*, 646–657.

(21) Hurd, C. D.; Gershbein, L. L. *J. Am. Chem. Soc.* **1947**, *69*, 2328–2335.

(22) Hoyle, C. E.; Bowman, C. N. *Angew. Chem. Int. Ed.* **2010**, *49*, 1540–1573.

(23) Bader, H.; Cross, L. C.; Heilbron, I.; Jones, E. R. H. *J. Chem. Soc.* **1949**, 619–623.

(24) Fairbanks, B. D.; Scott, T. F.; Kloxin, C. J.; Anseth, K. S.; Bowman, C. N. *Macromolecules* **2009**, *42*, 211–217.

(25) Diels, O.; Alder, K. *Liebigs Ann. Chem.* **1928**, *460*, 98–122.

(26) Sauer, J.; Sustman, R. *Angew. Chem. Int. Ed. Engl.* **1980**, *19*, 779–807.

(27) Mukaiyama, T.; Hoshino, T. *J. Am. Chem. Soc.* **1960**, *82*, 5339–5342.

(28) Huisgen, R. *Angew. Chem. Int. Ed.* **1963**, *2*, 565–632.

(29) Parker, R. E.; Isaacs, N. S. *Chem. Rev.* **1959**, *59*, 737–799.

(30) Agard, N. J.; Prescher, J. A.; Bertozzi, C. R. *J. Am. Chem. Soc.* **2004**, *126*, 15046–15047.

(31) Jewett, J. C.; Sletten, E. M.; Bertozzi, C. R. *J. Am. Chem. Soc.* **2010**, *132*, 3688–3690.

(32) Carboni, R. A.; Lindsey, R. V. *J. Am. Chem. Soc.* **1959**, *81*, 4342–4346.

(33) Johnson, J. A.; Finn, M. G.; Koberstein, J. T.; Turro, N. J. *Macromol. Rapid Commun.* **2008**, *29*, 1052–1072.

(34) Kade, M. J.; Burke, D. J.; Hawker, C. J. *J. Polym. Sci. Part A: Polym. Chem.* **2010**, *48*, 743–750.

(35) Andrew B. Lowe, A. B.; Hoyle, C. E.; Bowman, C. N. *J. Mater. Chem.* **2010**, *20*, 4745–4750.

(36) Hoogenboom, R. *Angew. Chem. Int. Ed.* **2010**, *49*, 3415–3417.

(37) Zheng, Y.; Li, S.; Wenga, Z.;Gao, C. *Chem. Soc. Rev.* **2015**, *44*, 4091–4130.

(38) Cao, X. S.; Shi, Y.; Gao, H. F. *Synlett* **2017**, *28*, 391–396.

(39) Yamamoto, T. *Polym. J.* **2013**, *45*, 711–717.

(40) Josse, T.; Winter, J. D.; Gerbaux, P.; Coulembier, O. *Angew. Chem. Int. Ed.* **2016**, *55*, 13944–13958.

(41) Huang, Z. H.; Zhou, Y. Y.; Wang, Z. M.; Li, Y.; Zhang, W.; Zhou, N. C.; Zhang, Z. B.; Zhu, X. L. *Chin. J. Polym. Sci.* **2017**, *35*, 317–341.

(42) Barnes, J. C.; Ehrlich, D. J. C.; Gao, A. X; Leibfarth, F. A.; Jiang,Y.; Zhou, E.; Jamison, T. F.; Johnson, J. A. *Nat. Chem.* **2015**, *7*, 810–815.

(43) Fiers, G.; Chouikhi, D.; Oswald, L.; Ouahabi, A. A.; Chan-Seng, D.; Charles, L.; Lutz, J. F. *Chem. Eur. J.* **2016**, *22*, 17945–17948.

(44) Huang, Z.; Zhao, J.; Wang, Z.; Meng, F.; Ding, K.; Pan, X.; Zhou, N.; Li, X.; Zhang, Z.; Zhu, X. *Angew. Chem. Int. Ed.* **2017**, *56*, 13612–13617.

(45) Song, B.; Lu, D.; Qin, A.; Tang, B. Z. *J. Am. Chem. Soc.* **2022**, *144*, 1672–1680.

Chapter 2

Mechanical Properties of Network Polymers Formed from Monodisperse Oligo(ethylene glycol)s of Different Molecular Weights through Thiol–Yne Reaction

2-1. Introduction

Network polymers are an important class of polymers acting as resins, elastomers, and gels, and are thus utilized in a wide variety of fields, e.g., building materials, civil engineering, automotive industry, electrical industry, and biomedical applications.[1–5] Network polymers are usually prepared by (1) crosslinking of linear polymers or by (2) copolymerization of multifunctional monomers.[6] A typical example of (1) is vulcanization of natural rubber, while (2) includes copolymerization of vinyl and divinyl monomers. However, these methods usually yield heterogeneous network polymers, in which densely-crosslinked and loosely-crosslinked networks coexist.[7–9] Such heterogeneity prevents uniform stress distribution in the network polymer and causes poor mechanical properties and swelling characteristics.

To prepare homogeneous network polymer, some research groups have reported coupling of branched polymers possessing reactive groups at the chain ends. Sakai et al.[10–12] have coupled four-arm star-shaped poly(ethylene glycol)s (tetra-PEG) possessing

amino and *N*-hydroxysuccinimide terminals through amide formation to obtain a homogeneous network polymer containing solvents, which is called “tetra-PEG gel”. The structure and mechanical properties of tetra-PEG gel have been well characterized to confirm the high uniformity and high mechanical strength of the gel. Other groups have also reported the formation of homogeneous network polymers using branched polymers crosslinked by click chemistry, e.g., copper(I)-catalyzed azide–alkyne cycloaddition (CuAAC),[13–16] thiol–ene reaction,[17–19] and thiol–yne reaction.[20–24] The network polymers obtained have been characterized by glass transition temperature and rheological measurements.[13–17,20–24]

Among the reactions for click chemistry, thiol–yne reaction forms branched structures, i.e., 1,2-dithioether, through the addition of two equivalents of thiol to one equivalent of alkyne (Scheme 2-1).[25–27] Thus, network polymers are prepared from dithiol and diyne compounds through the thiol–yne reaction.[28,29] The author focuses on this simple system for the preparation of homogeneous network polymers.

In this chapter, thiol–yne reaction is carried out using modified monodisperse oligo(ethylene glycol) (MD-OEG) samples with thiol and yne moieties on both ends to form homogeneous network polymers. The author also studies the effect of the degree of polymerization of MD-OEG on the mechanical properties of the network polymers

obtained. The thiol–yne reaction of similar components has been reported by Han et al. [30,31] for the formation of hyperbranch polymers, in which dilute conditions are utilized to avoid the formation of network polymers. In this study, however, the thiol–yne reaction is conducted under bulk conditions.

Scheme 2-1. Proposed Mechanism of Radical Thiol–Yne Reaction

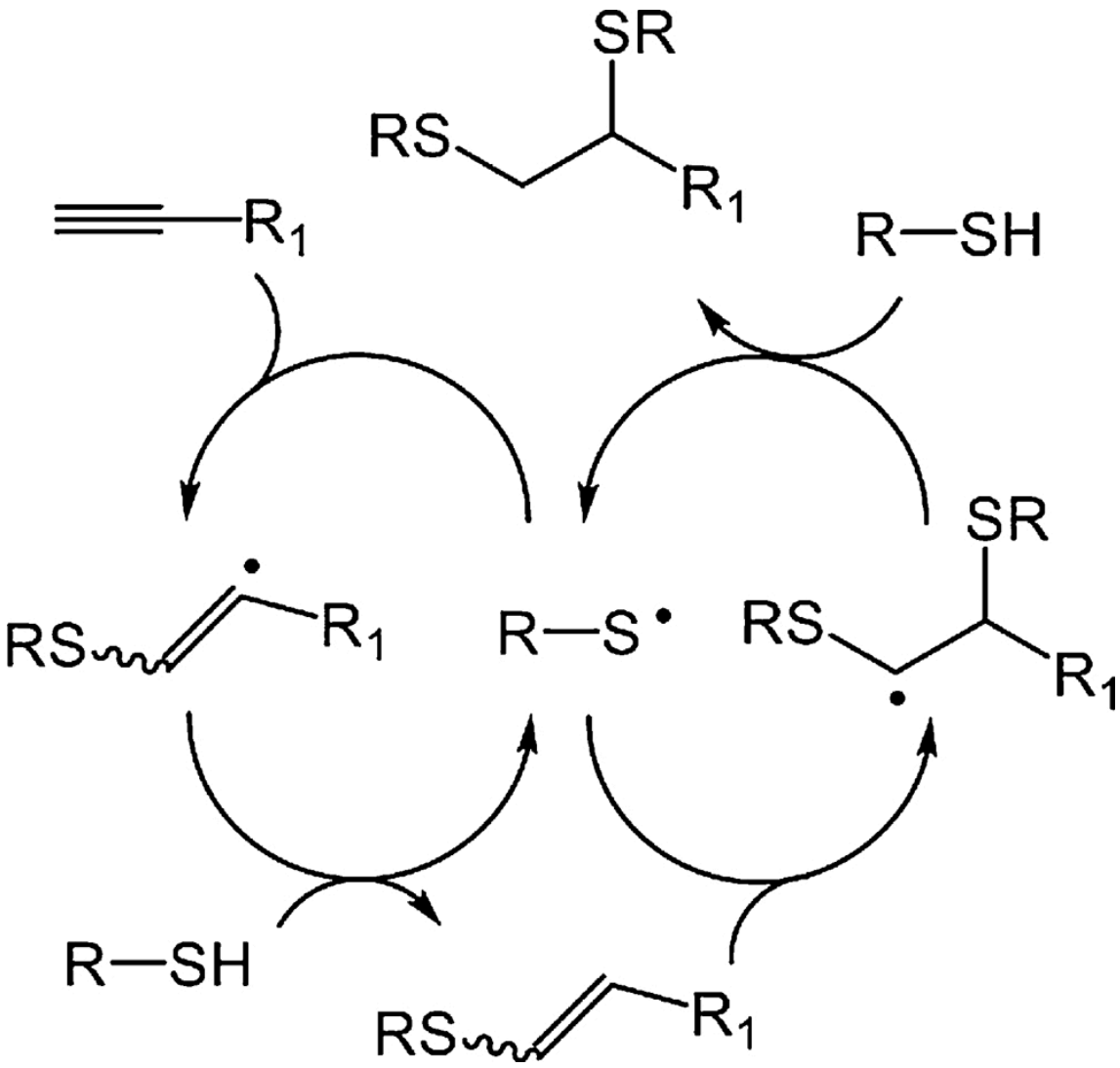

2-2 Experimental Section

Materials. Tetraethylene glycol and propargyl bromide solution (80 wt% in toluene) were purchased from Sigma-Aldrich (St. Louis, MO). Pyridine was purchased from FUJIFILM Wako Pure Chemical Corp. (Osaka, Japan). Ethanol was purchased from Shinwa Alcohol Industry (Chiba, Japan). IRGACURE® 184 was purchased from BASF Japan Ltd. (Tokyo, Japan). 3,6-Dioxa-1,8-dithiol (DT-EG2), pentaethylene glycol, and phosphorus tribromide (PBr_3) were purchased from Tokyo Chemical Industry Co., Ltd. (Tokyo, Japan). Thiourea, 35% hydrochloric acid, sodium hydroxide (NaOH), potassium hydroxide (KOH), anhydrous sodium sulfate (Na_2SO_4), dichloromethane, and methanol were purchased from Nacalai Tesque Inc. (Kyoto, Japan). All reagents were used as received. For thin layer chromatography (TLC) analysis through this work, Merck precoated TLC plates (silica gel 60 F254) were used. Silica gel 60 (Nacalai Tesque, spherical, neutrality) was used for purification of the products by column chromatography.

Measurements. ^1H NMR spectra were recorded on a JEOL JNM ECS400 spectrometer using $CDCl_3$ as solvent. Tetramethylsilane (TMS) was used as an internal standard. Electrospray ionization mass spectra (ESI-MS) were obtained in a positive ion mode on a Thermo Fisher Scientific LTQ Orbitrap-XL, controlled by the XCARIBUR 2.1 software package. Methanol was used as a solvent. The condition of ionization was

set to the following parameters; ion spray voltage at 3.5 kV, ion spray temperature at 100 °C, and ion transfer tube temperature at 275 °C. Internal calibration of ESI-MS was performed using the monoisotopic peaks of sodium adducted ion of diethylphthalate (*m*/*z* 314.1410), protonated ion of di-2-ethylhexylphthalate (*m*/*z* 391.2843), and sodium adducted ion of di-2-ethylhexyl-phthalate (*m*/*z* 413.2662). IR spectra were recorded on a JASCO FT/IR 6100 spectrometer using a sample sandwiched with CaF_2 plates and a poly(tetrafluoroethylene) (PTFE) spacer of 100 μm in thickness. Compression tests were carried out with a RHEONERII creep meter (model: RE2-33005B, Yamaden Co., Ltd., Tokyo, Japan).

Preparation of Dibromides of Monodisperse Oligo(ethylene glycol) (DBr-EG*n*). A typical example of the preparation of DBr-EG*n* is described below.[32,33]

PBr_3 (2.00 mL, 21.1 mmol) was slowly added to a mixture of tetraethylene glycol (4.00 mL, 23.3 mmol) and pyridine (1.5 mL) with stirring at 0 °C. The reaction was allowed to proceed at room temperature for two days. Water (10 mL) was added to the mixture and the product was extracted with dichloromethane (4 × 50 mL). The organic layers were combined. The combined organic phase was washed with saturated aqueous NaCl (2 × 100 mL) and dried over Na_2SO_4. After filtration, the solvent was removed under reduced pressure to obtain DBr-EG3 as a colorless oil (6.19 g, 83%). ^{1}H NMR (400

MHz, 298 K, $CDCl_3$): δ 3.82 (t, J = 6.4 Hz, 4H), 3.68 (s, 8H), 3.47 (t, J = 6.4 Hz, 4H). HRMS (ESI) m/z: $[M + Na]^+$ calcd for $C_8H_{16}Br_2NaO_3$ 342.9338; found 342.9330.

Using pentaethylene glycol (4.00 mL, 19.0 mmol) and PBr_3 (2.00 mL, 21.1 mmol), DBr-EG4 was obtained as a colorless oil (5.66 g, 82 %). ^1H NMR (400 MHz, 298 K, $CDCl_3$): δ 3.81 (t, J = 6.4 Hz, 4H), 3.67 (s, 12H), 3.48 (t, J = 6.4 Hz, 4H). HRMS (ESI) m/z: $[M + Na]^+$ calcd for $C_{10}H_{20}Br_2NaO_4$ 386.9600; found 386.9600.

Preparation of Dithiols of Monodisperse Oligo(ethylene glycol) (DT-EG*n*). A typical example of the preparation of DT-EG*n* is described below.[32,33]

Thiourea (15.0 g, 197 mmol) was dissolved in ethanol (100 mL) under reflux. DBr-EG3 (6.19 g, 19.3 mmol) was added dropwise to this solution, and the reaction was allowed to proceed under reflux overnight. The solvent was then removed under reduced pressure. To the residue, aqueous NaOH (20%, 160 mL) was added and the mixture was heated under reflux for 5 h. After cooling, a small amount of 15% hydrochloric acid was slowly added to adjust the pH to ca. 1. The product was extracted with dichloromethane (4 × 200 mL). The organic layers were combined. The combined organic phase was washed with water (500 mL) and dried over anhydrous Na_2SO_4. After filtration, the solvent was removed under reduced pressure to obtain pale yellow oil. The product was purified by column chromatography using a mixed solvent of hexane and ethyl acetate

(1/1, v/v) to obtain DT-EG3 as a colorless oil (2.01 g, 46%). ^{1}H NMR (400 MHz, 298 K, $CDCl_3$): δ 3.68–3.63 (m, 8H), 3.63 (t, J = 6.4 Hz, 4H), 2.70 (dt, J = 8.2, 6.4 Hz, 4H), 1.60 (t, J = 8.2 Hz, 2H). HRMS (ESI) m/z: $[M - 2H + Na]^+$ calcd for $C_8H_{16}NaO_3S_2$ 247.0439; found 247.0432.

Using DBr-EG4 (5.82 g, 16.0 mmol) and thiourea (12.5 g, 164 mmol), DT-EG4 was obtained as a colorless oil (2.51 g, 58 %). ^{1}H NMR (400 MHz, $CDCl_3$): δ 3.66–3.62 (m, 12 H), 3.62 (t, J = 6.4 Hz, 4H), 2.70 (dt, J = 8.2, 6.4 Hz, 4H), 1.59 (t, J = 8.2 Hz, 2H). HRMS (ESI) m/z: $[M + Na]^+$ calcd for $C_{10}H_{24}NaO_4S_2$ 293.0852; found 293.0851.

Preparation of Diynes of Monodisperse Oligo(ethylene glycol) (DY-EG*n*). A typical example of the preparation of DY-EG*n* is described below.[30]

DT-EG2 (0.91 g, 5.00 mmol) was dissolved in methanol (5 mL). To this solution, a solution of KOH (0.83 g, 14.9 mmol) in methanol (5 mL) was added dropwise with vigorous stirring. The mixture was cooled with an ice-water bath, and then propargyl bromide (80 wt% in toluene, 2.30 mL, 21.2 mmol) was added to the mixture. After stirring overnight, the solvent was removed under reduced pressure. The residue was dissolved in dichloromethane (50 mL) and washed with saturated aqueous NaCl (2 × 50 mL). The solution was dried over anhydrous Na_2SO_4. After filtration, the solvent was removed under reduced pressure to obtain orange oil. The product, DY-EG2, was purified by

column chromatography using a mixed solvent of hexane and ethyl acetate (2/1, v/v). After evaporation of the solvent, DY-EG2 was obtained as a yellow oil (0.96 g, 75 %). ^{1}H NMR (400 MHz, 298 K, $CDCl_3$): δ 3.73 (t, J = 6.6 Hz, 4H), 3.64 (s, 4 H), 3.33 (d, J = 2.6 Hz, 4H), 2.90 (t, J = 6.6 Hz, 4H), 2.24 (t, J = 2.6 Hz, 2H). HRMS (ESI) m/z: $[M + Na]^+$ calcd for $C_{12}H_{18}NaO_2S_2$ 281.0646; found 281.0638.

Using DT-EG3 (1.14 g, 5.02 mmol) and propargyl bromide (80 wt. % in toluene, 2.30 mL, 21.2 mmol), DY-EG3 was obtained as a yellow oil (0.86 g, 57 %). ^{1}H NMR (400 MHz, 298 K, $CDCl_3$): δ 3.72 (t, J = 6.6 Hz, 4H), 3.69–3.63 (m, 8H), 3.32 (d, J = 2.6 Hz, 4H), 2.89 (t, J = 6.6 Hz, 4H), 2.24 (t, J = 2.6 Hz, 2H). HRMS (ESI) m/z: $[M + Na]^+$ calcd for $C_{14}H_{22}NaO_3S_2$ 325.0908; found 325.0901.

Using DT-EG4 (2.13 g, 7.88 mmol) and propargyl bromide (80 wt% in toluene, 6.50 mL, 59.8 mmol), DY-EG4 was obtained as a yellow oil (1.87 g, 68 %). ^{1}H NMR (400 MHz, 298 K, $CDCl_3$): δ 3.72 (t, J = 6.6 Hz, 4H), 3.68–3.63 (m, 12H), 3.32 (d, J = 2.6 Hz, 4H), 2.90 (t, J = 6.6 Hz, 4H), 2.24 (t, J = 2.6 Hz, 2H). HRMS (ESI) m/z: $[M + Na]^+$ calcd for $C_{16}H_{26}NaO_4S_2$ 369.1165; found 369.1165.

Kinetic Analysis of Thiol–Yne Reaction Using Time-Dependent IR Spectroscopy. Kinetic analysis of thiol–yne reaction was carried out by time-dependent IR spectroscopy according to the procedure of Senyurt et al.[17] with a slight modification.

A typical procedure is described below.

DT-EG3 (228 mg, 1.01 mmol), DY-EG3 (150 mg, 0.50 mmol), and IRGACURE® 184 (15 mg, 75 μmol) were mixed under a nitrogen atmosphere. The mixture was sandwiched with two CaF_2 plates using a 100-μm thick PTFE spacer. An LED lamp (POT-365, Asahi Spectra Co., Ltd., Tokyo, Japan) was used as the light source, and the distance between the light source and the sample was fixed at 2.5 cm. FT-IR spectra of the sample were recorded on a JASCO FT/IR 6100 spectrometer after every five seconds of irradiation with 365 nm UV light.

Preparation of Network Polymer Samples for Compression Tests. A typical example of the preparation of the samples for compression tests is described below.

DT-EG3 (228 mg, 1.01 mmol), DY-EG3 (150 mg, 0.50 mmol), and IRGACURE® 184 (15 mg, 75 μmol) were mixed under a nitrogen atmosphere. The mixture was placed in a 1.0-mm thick silicone mold and sandwiched with two glass plates. The sample was irradiated with 365 nm UV light using an LED lamp (POT-365, Asahi Spectra Co., Ltd., Tokyo, Japan) for predetermined times. The distance between the light source and the sample was fixed at 1.5 cm.

2-3 Results and Discussion

Preparation of DT-EG*n* and DY-EG*n*. Aiming at easy formation of homogeneous network polymers, the author synthesized network polymers from monodisperse oligo(ethylene glycol) (MD-OEG) through thiol–yne reaction. The author prepared dithiols and diynes (DT-EG*n* and DY-EG*n*, where *n* denotes the degree of polymerization (DP)) using MD-OEG samples of different DP as starting materials, according to Scheme 2-1. The MD-OEG samples were first brominated at both hydroxy terminals, and then treated with thiourea to yield DT-EG*n* samples. The DT-EG*n* samples were coupled with propargyl bromide under basic conditions to produce DY-EG*n* samples. (Commercially available DT-EG2 was used.) All the DT-EG*n* and DY-EG*n* samples of *n* = 2, 3, and 4 were characterized by ^{1}H NMR and MS (see Experimental Section and Figure 2-1), and their purities were confirmed to be high enough for the following experiments.

Scheme 2-2. Preparation of DT-EG*n* and DY-EG*n* Samples

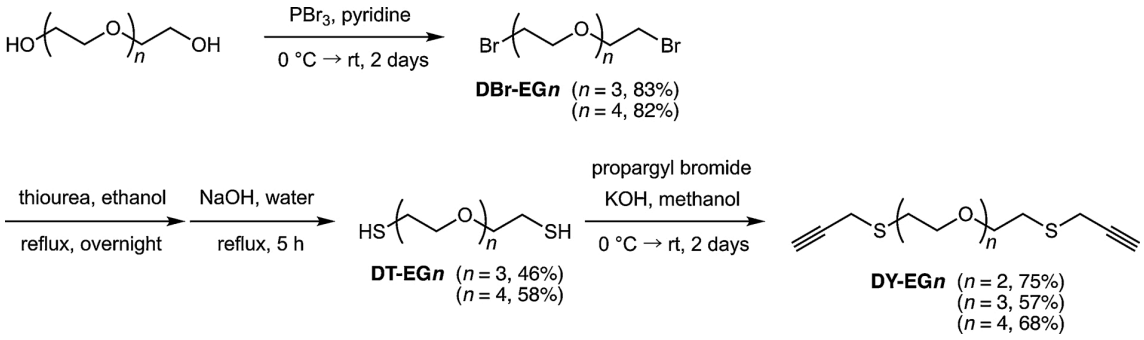

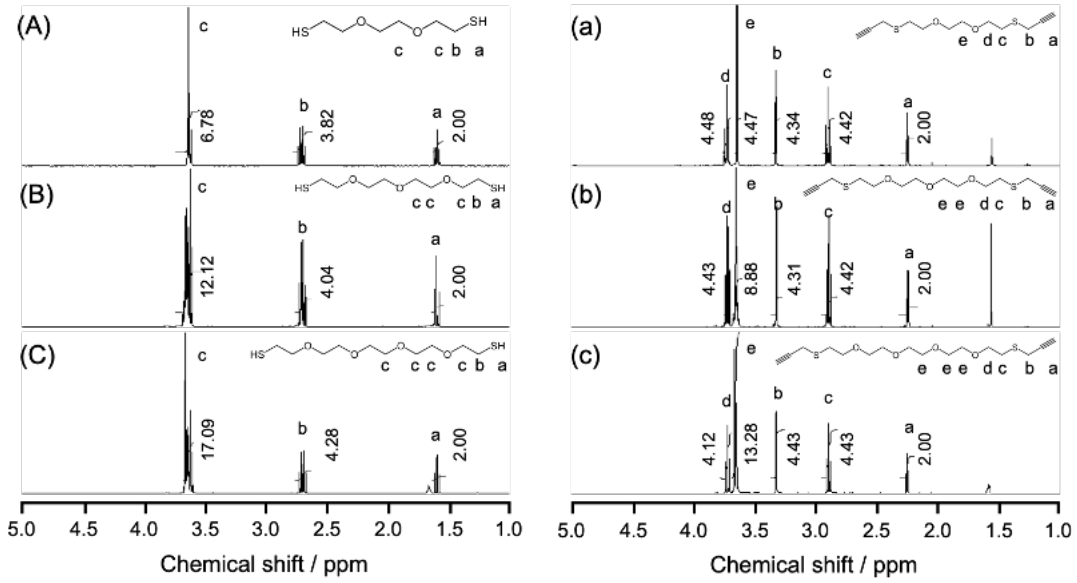

Figure 2-1. ^{1}H NMR spectra for DT-EG2 (A), DT-EG3 (B), DT-EG4 (C), DY-EG2 (a), DY-EG3 (b), and DY-EG4 (c) in $CDCl_3$.

Kinetic Analysis of Thiol–Yne Reaction of DT-EG*n* and DY-EG*n*. In this study, the author compares the mechanical properties of the network polymer samples formed by the thiol–yne reaction of DT-EG*n* and DY-EG*n* samples of different DP

(Scheme 2-3). If the efficiency of thiol–yne reaction alters considerably for different *n*, one has to take into account the different reaction efficiencies when discuss the *n* dependency of mechanical properties of the network polymers. Thus, the author has started this study with kinetic analysis of the thiol–yne reactions of DT-EG*n* and DY-EG*n* samples of different *n*, through IR measurements of thin films.[17] IR spectra were obtained for each sample after every five-second UV irradiation, as can be seen in Figure 2-2. Before UV irradiation, all the IR spectra for n = 2, 3, and 4 exhibit absorption bands assignable to the stretching vibration of thiol and yne at 2555 and 2115 cm^{-1}, respectively. (It was not possible to assign absorption bands to the vinyl sulfide in these spectra.) The intensity of both absorption bands became weaker as the irradiation time was increased. After 60 s, the absorption bands almost disappeared. These observations indicate that the thiol–yne reaction completes within 60 s under the given conditions.

Scheme 2-3. Preparation of Network Polymers from DT-EG*n* and DY-EG*n* Through the Thiol–Yne Reaction

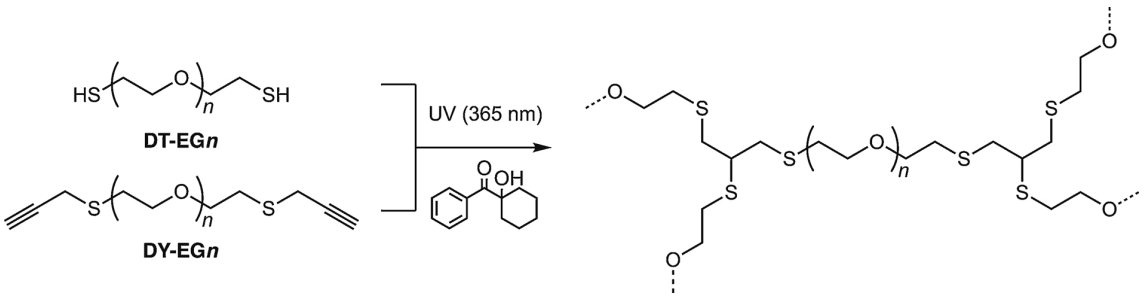

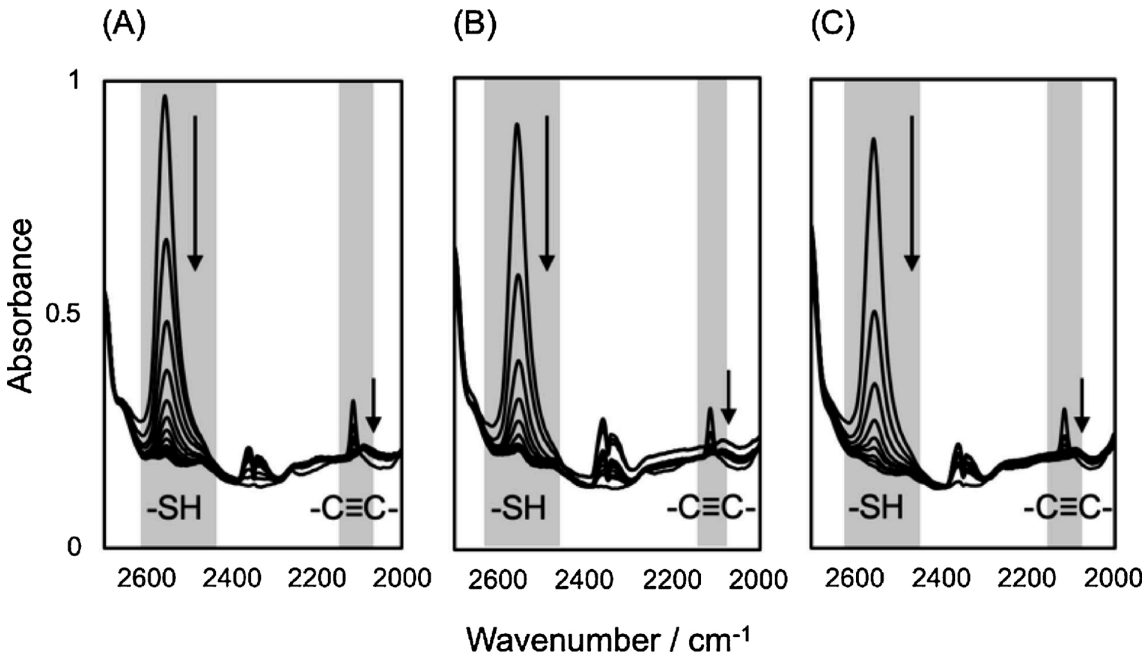

Figure 2-2. IR spectra for mixtures of DT-EG*n*, DY-EG*n*, and IRGACURE® 184 under UV irradiation at different irradiation times; *n* =2 (A), 3 (B), and 4 (C).

Since these IR spectra demonstrate that the thiol–yne reaction was completed for *n* = 2, 3, and 4, one can compare directly the mechanical properties of the network polymers of different *n* in the following subsections. Since the initial concentrations of DT-EG*n* and DY-EG*n* were known, the concentrations of DT-EG*n* and DY-EG*n* at time *t* were calculated from the absorbances of bands due to the thiol and yne moieties, and plotted against the total irradiation times as shown in Figure 2-3. In all the cases of *n* = 2, 3, and 4, the concentration decreased to zero within 60 s. On the basis of the previous works on kinetic analysis of thiol–yne reaction,[20,21] the author evaluated the apparent rate

constants of the present thiol–yne reaction using a simplified model as proposed below.

The addition of thiol to yne and the subsequent addition of thiol to vinyl sulfide proceed, according to Scheme 2-1. Given that [C ≡ C], [C = C], and [C − C] are the concentrations of yne, vinyl sulfide, and 1,2-dithioether, respectively, one can write the following equations.

$$\frac{d[\mathrm{C} \equiv \mathrm{C}]}{dt} = -k_1[\mathrm{S}\bullet][\mathrm{C} \equiv \mathrm{C}] \tag{2-1}$$

$$\frac{d[\mathrm{C} = \mathrm{C}]}{dt} = k_1[\mathrm{S}\bullet][\mathrm{C} \equiv \mathrm{C}] - k_2[\mathrm{S}\bullet][\mathrm{C} = \mathrm{C}] \tag{2-2}$$

$$\frac{d[\mathrm{C} - \mathrm{C}]}{dt} = k_2[\mathrm{S}\bullet][\mathrm{C} = \mathrm{C}] \tag{2-3}$$

where k_1 and k_2 are the reaction constants for addition of a thiyl radical to alkyne and vinyl sulfide, respectively, and [S•] is the concentration of thiyl radical. From the conservation of mass,

$$[\mathrm{C} \equiv \mathrm{C}]_0 = [\mathrm{C} \equiv \mathrm{C}] + [\mathrm{C} = \mathrm{C}] + [\mathrm{C} - \mathrm{C}] \tag{2-4}$$

where $[\mathrm{C} \equiv \mathrm{C}]_0$ is the initial concentration of yne. Given the steady state conditions for [S•], eqs 2-1, 2-2, and 2-3 are rewritten as

$$\frac{d[\mathrm{C} \equiv \mathrm{C}]}{dt} = -k_1'[\mathrm{C} \equiv \mathrm{C}] \tag{2-5}$$

$$\frac{d[\mathrm{C} = \mathrm{C}]}{dt} = k_1'[\mathrm{C} \equiv \mathrm{C}] - k_2'[\mathrm{C} = \mathrm{C}] \tag{2-6}$$

$$\frac{d[\mathrm{C} - \mathrm{C}]}{dt} = k_2'[\mathrm{C} = \mathrm{C}] \tag{2-7}$$

where k_1' (= k_1[S•]) and k_2' (= k_2[S•]) are apparent rate constants. From eqs 2-4, 2-5, 2-6,

and 2-7, [C ≡ C], [C = C], and [C − C] are calculated as

$$[\mathrm{C} \equiv \mathrm{C}] = [\mathrm{C} \equiv \mathrm{C}]_0 \exp(-k_1' t) \tag{2-8}$$

$$[\mathrm{C} = \mathrm{C}] = \frac{k_2'}{k_2' - k_1'}[\mathrm{C} \equiv \mathrm{C}]_0\{\exp(-k_1' \mathrm{t}) - \exp(-k_2' \mathrm{t})\} \tag{2-9}$$

$$[\mathrm{C} - \mathrm{C}] = [\mathrm{C} \equiv \mathrm{C}]_0 - ([\mathrm{C} \equiv \mathrm{C}] + [\mathrm{C} = \mathrm{C}]) \tag{2-10}$$

The thiol concentration [SH] can be also calculated as

$$[\mathrm{SH}] = [\mathrm{SH}]_0 - ([\mathrm{C} \equiv \mathrm{C}]_0 - [\mathrm{C} \equiv \mathrm{C}]) - [\mathrm{C} - \mathrm{C}] \tag{2-11}$$

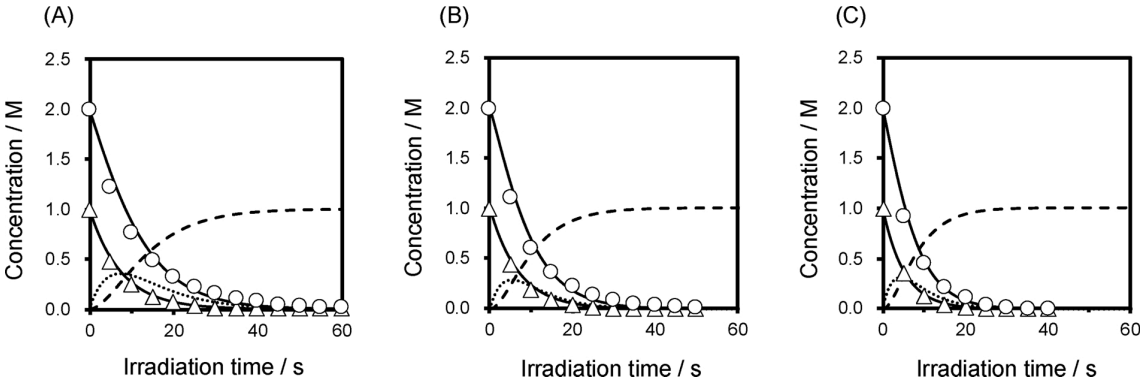

Figure 2-3. Time-evolutions of the concentrations of thiol (circle) and yne (triangle) during the thiol–yne reaction of mixtures of DT-EG*n*, DY-EG*n*, and IRGACURE® 184 under UV irradiation; *n* = 2 (A), 3 (B), and 4 (C). The molar ratio of DT-EG*n* and DY-EG*n* was fixed at 2:1 and 5 mol% of IRGACURE® 184 was used. The best-fitted curves of the concentrations of thiol (solid line), yne (solid line), vinyl sulfide (dotted line), and 1,2-dithioether (broken line) ([SH], [C ≡ C], [C = C], and [C – C], respectively) based on the simplified kinetic model are also drawn.

When the apparent rate constants (k_1' and k_2') are chosen appropriately, the estimated thiol and yne concentrations ([SH] and [C ≡ C], respectively) using eqs 2-11 and 2-8 agree with the experimental data as can be seen in Figure 2-3. Figure 2-4 displays the n dependencies of k_1' and k_2'. It should be noted that both k_1' and k_2' are apparent values, which contain the thiyl radical concentration ([S•]). Since the concentrations of photoinitiator, i.e., IRGACURE® 184, were almost the same in all the cases of n, it is likely that [S•] was virtually constant, i.e., independent of n. Thus, the values of k_1' and k_2' can be compared. Figure 2-4 shows that both k_1' and k_2' increase with n. The values of k_1' and k_2' are comparable for n = 2, whereas k_2' is larger than k_1' for n = 3 and 4. Since the activation enthalpies of thiol–yne reaction should be almost the same for n = 2, 3, and 4, the difference in k_1' and k_2' may be ascribable to a difference in the activation entropy of the reaction. This observation indicates that the terminal thiol and yne moieties are more mobile at a larger n because of the greater flexibility of longer OEG chain.

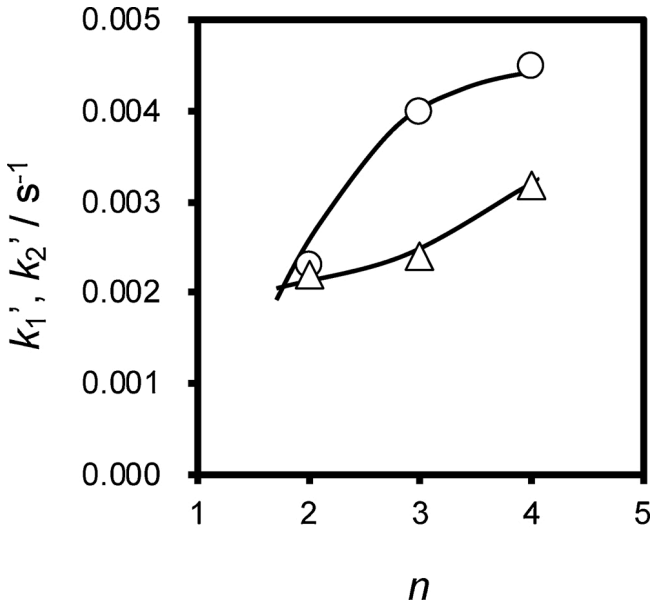

Figure 2-4. The n dependencies of apparent rate constants, k_1' (triangle) and k_2' (circle), of the thiol–yne reaction of DT-EG*n* and DY-EG*n* under UV irradiation.

Mechanical Properties of Network Polymers Formed from DT-EG*n* and DY-EG*n*. The samples for measurements of mechanical properties were prepared as follows. Since the light source used in this study (a POT-36 LED lamp) can irradiate only a circular area of φ = 12 mm, disk-shaped specimens of network polymers were prepared for compression tests. The specimens were prepared from mixtures of DT-EG*n*, DY-EG*n*, and IRGACURE® 184 using a silicone mold sandwiched with two glass slides under UV irradiation for different irradiation times. Their mechanical properties were then investigated by compression tests with a creep meter. Figure 2-5 displays a typical example of stress–strain curves for the disk-shaped specimens of network polymers. From

the initial slopes in Figure 2-5, values of Young's modulus (E) for n = 2, 3, and 4 were estimated, and the average E values for three different samples prepared under the same conditions were plotted in Figure 2-6 against the irradiation time. In the cases of n =2 and 3, E increased with the irradiation time and then leveled off at irradiation times longer than 60 min. In the case of n = 4, on the other hand, E was almost constant at irradiation times longer than 10 min.

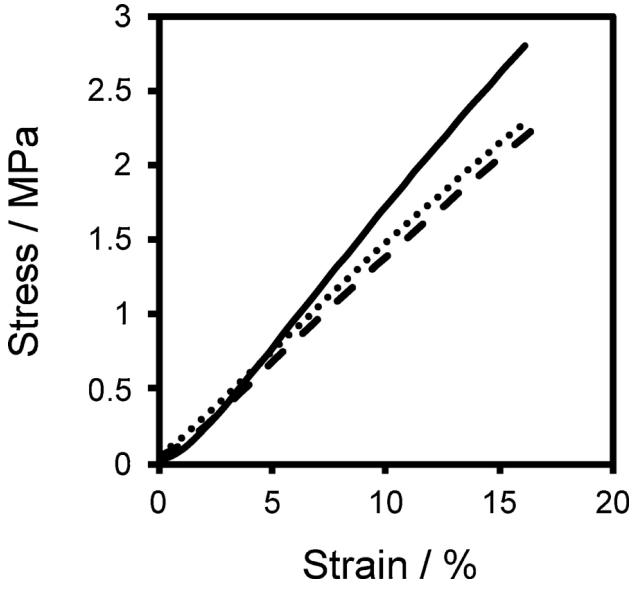

Figure 2-5. Stress–strain curves obtained from the compression tests for network polymers of n = 2 (solid line), 3 (dotted line), 4 (broken line).

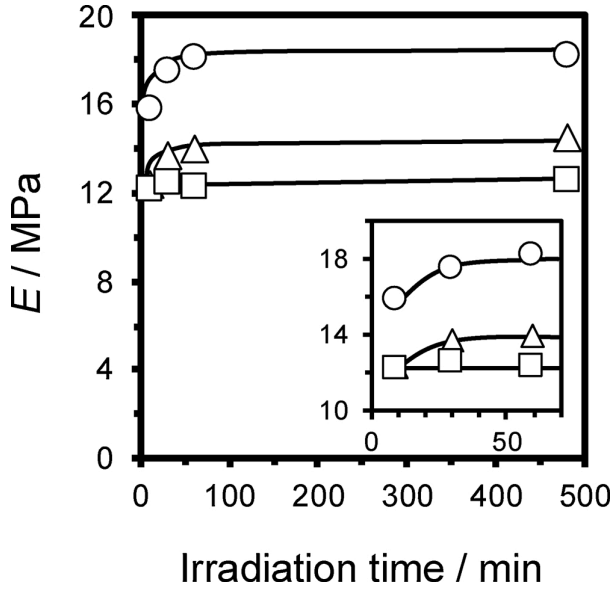

Figure 2-6. Young's modulus of the network polymers as a function of the irradiation time for n = 2 (circle), 3 (triangle), and 4 (square).

Figure 2-7 indicates the saturated E (E_{sat}) as a function of n. As can be seen in this figure, E_{sat} decreased from 18.2 to 12.6 MPa with increasing n from 2 to 4. This is because the crosslinking density decreased with increasing n. The chain length between crosslinks was comparable to the statistical segment length of PEG (ca. 0.8 nm[34,35]) in this study. It is still an open question to predict Young's modulus for such a case.[36] Thus, here the author compares preliminarily the E_{sat} data with the rubber elasticity theory. On the basis of the affine network model, Young's modulus E is given by

$$E = \frac{3\rho \mathrm{RT}}{M_{net}} \tag{2-12}$$

where ρ, R, T, and M_{net} denote the polymer density, the gas constant, the absolute

temperature, and the molecular weight between crosslinking points, respectively. The experimental E_{sat} values were compared with the estimated E values as can be seen in Figure 2-8. The ratio of the experimental and estimated values of E is almost constant at ca. 45% independent of n. This ratio corresponds to the efficiency of formation of mechanically active chains. Mechanically inactive chains may be formed statistically by the formation of loops and dangling chains, which should be formed by minor side reactions on the thiol and yne moieties. These observations indicate that the probability of formation of mechanically active (or inactive) chains is almost constant independent of n in the n range examined in this study.

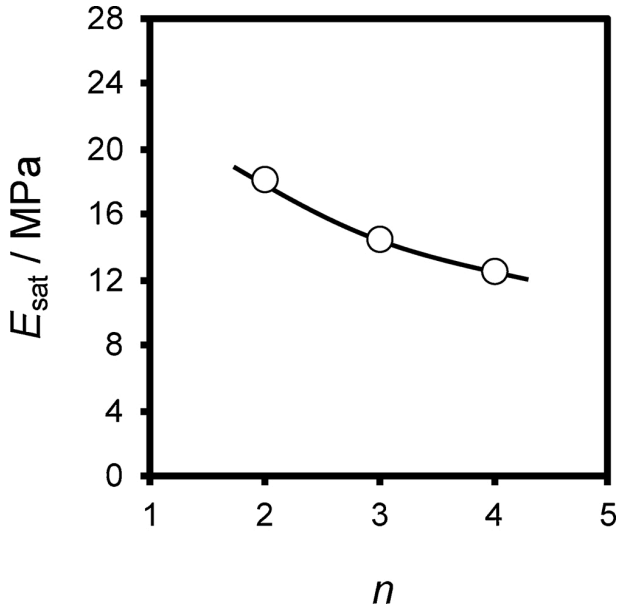

Figure 2-7. The experimental Young's modulus (E_{sat}) as a function of n for the network polymers.

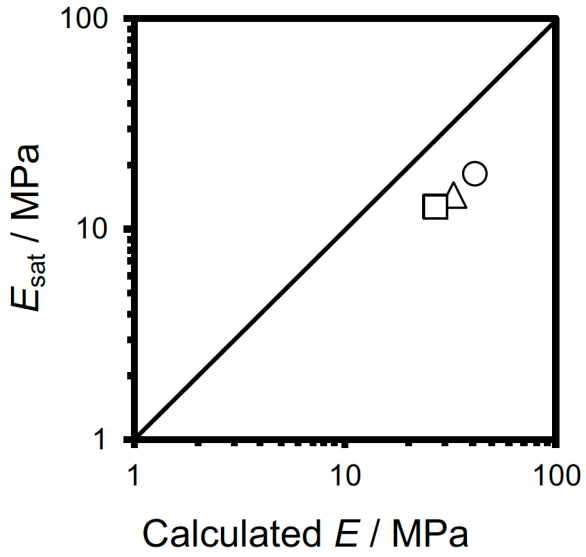

Figure 2-8. The experimental and calculated values of Young's modulus E for the network polymers of n = 2 (circle), 3 (triangle), and 4 (square).

2-4. Conclusions

In this study, the author synthesized network polymers from monodisperse DT-EG*n* and DY-EG*n* samples through the thiol–yne reaction to study the effect of *n* on the mechanical properties. The author first carried out kinetic analysis of the thiol–yne reaction of DT-EG*n* and DY-EG*n* samples of different *n* through IR measurements of thin films. The IR spectra indicated that the thiol–yne reaction completed within 60 s under the given conditions. On the basis of a simplified kinetic model proposed herein, the author estimated the apparent reaction rate constants, k_1' and k_2', for the thiol–yne reaction.

Both k_1' and k_2' increased with n, indicating that the terminal thiol and yne moieties were more mobile at a larger n. Based on the stress–strain curves obtained from compression tests, the saturated E (E_{sat}) decreased from 18.2 to 12.6 Pa with increasing n from 2 to 4 because of the decrease in crosslinking density with increasing n. The ratio of experimental E_{sat} and the E calculated based on the affine network model was almost constant at ca. 45% independent of n. These observations indicated that the probability of formation of mechanically active (or inactive) chains was almost constant independent of n in the n range examined in this study. Since the network polymer samples obtained in this study show Young's moduli higher than 10 MPa and contain rather high contents of sulfur atoms which increase the reflective index, the samples may be promising in some applications, e.g., adhesives and optical lenses.

2-5. References

(1) Rubinstein, M.; Colby, R. H. *Polymer Physics*; Oxford University Press: New York, 2003.

(2) Tanaka, F. *Polymer Physics: Applications to Molecular Association and Thermoreversible Gelation*; Cambridge University Press: Cambridge, 2011.

(3) Pascault, J.-P.; Sautereau, H.; Verdu, J.; Williams, R. J. J. *Thermosetting Polymers*; Marcel Dekker: New York, 2002.

(4) Mark, J. E.; Erman, B. *Rubberlike Elasticity: A Molecular Primer*, 2 ed.; Cambridge University Press: Cambridge, 2007.

(5) Osada, Y.; Khokholov, A. R. *Polymer Gels and Networks*; Marcel Dekker: New York, 2002.

(6) Mandal, B. M. *Fundamentals of Polymerization*; World Scientific Publishing: Singapore, 2011.

(7) Hecht, A. M.; Duplessix, R.; Geissler, E. *Macromolecules* **1985**, *18*, 2167–2173.

(8) Shibayama, M. *Macromol. Chem. Phys.* **1998**, *199*, 1–30.

(9) Seiffert, S. *Polym. Chem.* **2017**, *8*, 4472–4487.

(10) Sakai, T.; Matsunaga, T.; Yamamoto, Y.; Ito, C.; Yoshida, R.; Suzuki, S.; Sasaki, N.; Shibayama, M.; Chung, U.-i. *Macromolecules* **2008**, *41*, 5379–5384.

(11) Sakai, T. *React. Funct. Polym.* **2013**, *73*, 898–903.

(12) Sakai, T. *Polym. J.* **2014**, *46*, 517–523.

(13) Johnson, J. A.; Finn, M. G.; Koberstein, J. T.; Turro, N. J. *Macromol. Rapid Commun.* **2008**, *29*, 1052–1072.

(14) McBride, M. K.; Gong, T.; Nair, D. P.; Bowman, C. N. *Polymer* **2014**, *55*, 5880–5884.

(15) Oshima, K.; Fujimoto, T; Minami, E.; Mitsukami, Y. *Macromolecules* **2014**, *47*,

7573–7580.

(16) Oshima, K.; Mitsukami, Y. *Polymer* **2016**, *100*, 134–142.

(17) Senyurt, A. F.; Wei, H.; Hoyle, C. E.; Piland, S. G.; Gould, T. E. *Macromolecules* **2007**, *40*, 4901–4909.

(18) Hoyle, C. E.; Bowman, C. N. *Angew. Chem., Int. Ed.* **2010**, *49*, 1540–1573.

(19) Kade, M. J.; Burke, D. J.; Hawker, C. J. *J. Polym. Sci. Part A: Polym. Chem.* **2010**, *48*, 743–750.

(20) Fairbanks, B. D.; Scott, T. F.; Kloxin, C. J.; Anseth, K. S.; Bowman, C. N. *Macromolecules* **2009**, *42*, 211–217.

(21) Fairbanks, B. D.; Sims, E. A.; Anseth, K. S.; Bowman, C. N. *Macromolecules* **2010**, *43*, 4113–4119.

(22) Chan, J. W.; Shin, J.; Hoyle, C. E.; Bowman, C. N.; Lowe, A. B. *Macromolecules* **2010**, *43*, 4937–4942.

(23) Ganivada, M. N.; Kumar, P.; Shunmugam, R. *RSC Adv.* **2015**, *5*, 50001–50004.

(24) Oesterreicher, A.; Gorsche, C.; Ayalur-Karunakaran, S.; Moser, A.; Edler, M.; Pinter, G.; Schlögl, S.; Liska, R.; Griesser, T. *Macromol. Rapid Commun.* **2016**, *37*, 1701–1706.

(25) Hoogenboom, R. *Angew. Chem., Int. Ed.* **2010**, *49*, 3415–3417.

(26) Lowe, A. B.; Hoyle, C. E.; Bowman, C. N. *J. Mater. Chem.* **2010**, *20*, 4745–4750.

(27) Lowe, A. B. *Polymer* **2014**, *55*, 5517–5549.

(28) Chan, J. W.; Zhou, H.; Hoyle, C. E.; Lowe, A. B. *Chem. Mater.* **2009**, *21*, 1579–1585.

(29) Mano, Y.; Nagao, Y.; Takasu, A. *Polym. J.* **2014**, *46*, 682–6870.

(30) Han, J.; Zhao, B.; Tang, A.; Gao, Y.; Gao, C. *Polym. Chem.* **2012**, *3*, 1918–1925.

(31) Han, J.; Zheng, Y.; Zhao, B.; Li, S.; Zhang, Y.; Gao, C. *Sci. Rep.* **2014**, *4*, 4387.

(32) Bradshaw, J. S.; Krakowiak, K. E.; Izatt, R. M.; Bruening, R. L.; Tarbet, B. J. *J. Heterocycl. Chem.* **1990**, *27*, 347–349.

(33) Speziale, A. J. *Org. Synth.* **1950**, *30*, 35.

(34) Kienberger, F.; Pastushenko, V. P.; Kada, G.; Gruber, H. J.; Riener, C.; Schindler, H.; Hinterdorfer, P. *Single Molecules* **2000**, *1*, 123–128.

(35) Lee, H.; Venable, R. M.; MacKerell Jr, A. D.; Pastor, R. W. *Biophys. J.* **2008**, *95*, 1590–1599.

(36) Broedersz, C. P.; MacKintosh, F. C. *Rev. Mod. Phys.* **2014**, *86*, 995–1036.

Chapter 3

Synthesis of Interval-Controlled Cyclic Dimers by Click Chemistry

3-1. Introduction

Macrocycles, e.g., crown ether,[1] cyclodextrin,[2] and calixarene,[3] are an important class of nonlinear molecules, which are applicable to a wide range of fields, including catalyst chemistry and biomedical science, based on their molecular recognition ability.[4–6] Since macrocyclic structures in natural compounds often play an important role in biological activities, macrocycles are also used in pharmaceutical chemistry.[7,8] To expand the application fields, development of new type of macrocycles is of great importance. However, it is not easy to synthesize macrocyclic compounds because of entropically-disfavored ring-closing reaction. Click chemistry,[9] which is a technique for synthesis of functional molecules from simple building blocks by robust reactions, e.g., copper(I)-catalyzed azide–alkyne cycloaddition (CuAAC)[10,11] and thiol–ene reaction,[12,13] has been employed to synthesize macrocyclic interaction molecules. Binauld et al.[14] reported synthesis of uniform oligomers by stepwise CuAAC of triethylene glycol possessing azide and alkyne moieties. Cyclic oligomers were synthesized by CuAAC of the oligomers under highly dilute conditions. The author has focused on this simple approach to synthesize macrocyclic multivalent oligomers.

In this chapter, dialkyne possessing internal alkene for introduction of interacting moieties and diazide formed triethylene glycol are used. Macrocyclic dimers bearing adamantyl (Ad) and β-cyclodextrin (βCD) moieties are synthesized by stepwise CuAAC, followed by thiol–ene reaction.

3-2. Experimental Section

Materials. A propargyl bromide solution (80 wt% in toluene), 1-adamantanethiol, and anhydrous magnesium sulfate ($MgSO_4$) were purchased from Sigma-Aldrich (St. Louis, MO). *cis*-Butene-1,4-diol, *N*,*N*,*N*′,*N*″,*N*″-pentamethyldiethylenetriamine (PMDETA), 2,2-dimethoxy-2-phenylacetophenone (DMPA), and 6-amino-6-deoxy-β-cyclodextrin (NH_2-βCD) were purchased from Tokyo Chemical Industry Co., Ltd. (Tokyo, Japan). Triethylene glycol, *p*-toluenesulfonyl chloride, sodium hydride (60% suspension in paraffin liquid), thiourea, *N*,*N*′-dicyclohexylcarbodiimide (DCC), 1-hydroxybenzotriazole (HOBt), anhydrous sodium sulfate (Na_2SO_4), citric acid, tetra-sodium ethylenediaminetetraacetate (EDTA·4Na), sodium hydroxide (NaOH), sodium chloride (NaCl), triethylamine, hydrochloric acid (HCl), dimethyl sulfoxide (DMSO), *N*,*N*-dimethylformamide (DMF), dichloromethane, chloroform, and 1-butanol were purchased from Nacalai Tesque Inc. (Kyoto, Japan).

Sodium azide, copper(I) bromide (CuBr), diisopropyl azodicarboxylate (DIAD), triphenylphosphine, diphenylphosphoryl azide (DPPA), mercaptacetic acid, pyridine, acetone, diethyl ether, ethanol, ethyl acetate, hexane, tetrahydrofuran (THF), and methanol were purchased from FUJIFILM Wako Pure Chemical Corp. (Osaka, Japan). β-Cyclodextrin (βCD) was purchased from Junsei Chemical Co., Ltd (Tokyo, Japan). THF was distilled before use. Other reagents were used as received. For thin layer chromatography (TLC) analysis through this work, Merck precoated TLC plates (silica gel 60 F254) were used. Silica gel 60 (Nacalai Tesque, spherical, neutrality) was used for purification of the products by column chromatography.

Measurements. ^{1}H NMR spectra were recorded on a JEOL JNM ECS400 or ECA500 spectrometer using chloroform-*d* ($CDCl_3$), dimethyl sulfoxide-d (DMSO-d_6), or deuterium oxide (D_2O) as a solvent. Tetramethylsilane (TMS) was used as an internal standard for $CDCl_3$ and DMSO-d_6. Electrospray ionization mass spectra (ESI-MS) were obtained in a positive ion mode on a Thermo Fisher Scientific LTQ Orbitrap-XL, controlled by the XCARIBUR 2.1 software package. Methanol was used as a solvent. The condition of ionization was set to the following parameters; ion spray voltage at 3.5 kV, ion spray temperature at 100 °C, and ion transfer tube temperature at 275 °C. Internal calibration of ESI-MS was performed using the monoisotopic peaks of sodium adducted

ion of diethylphthalate (*m*/*z* 314.1410), protonated ion of di-2-ethylhexylphthalate (*m*/*z* 391.2843), and sodium adducted ion of di-2-ethylhexyl-phthalate (*m*/*z* 413.2662). Matrix-assisted laser desorption/ionization time-of-flight (MALDI-TOF) MS was conducted using a Shimadzu/KRATOS AXIMA-PERFORMANCE spectrometer with 4′-hydroxyazobenzene-2-carboxylic acid (HABA) as a matrix. TOF detection was performed using an appropriate accelerating voltage.

Preparation of Ditosylate of Triethylene Glycol (DTs-EG2).[15] Triethylene glycol (3.02 g, 20.1 mmol) was dissolved in pyridine (16 mL). To the solution, *p*-toluenesulfonyl chloride (8.88 g, 46.6 mmol) was added over 30 min in an ice-water bath. After stirring for 90 min at room temperature, the reaction mixture was poured into a mixture (150 mL) of ice and water to form colorless precipitate. The precipitate was recovered by filtration. DTs-EG2 was purified by recrystallization from ethanol and obtained as a colorless solid (7.17 g, 78 %). ^{1}H NMR (400 MHz, 298 K, $CDCl_3$): δ 7.79 (d, J = 8.2 Hz, 4H), 7.34 (d, J = 8.2 Hz, 4H), 4.14 (t, J = 9.6 Hz, 4H), 3.66 (t, J = 9.4, 4H), 3.53 (s, 4H), 2.45 (s, 6H).

Preparation of Diazide of Triethylene Glycol (DA-EG2).[16] DTs-EG2 (15.7g, 34.2 mmol) was dissolved in DMSO (200 mL). To the solution, sodium azide (7.05 g, 108 mmol) was added. After stirring at room temperature for 48 h, water (200 mL) was

added to the reaction mixture. The product was extracted from the aqueous solution with diethyl ether (3 × 100 mL). The organic layers were combined. The combined organic phase was washed with water (50 mL) and dried over Na_2SO_4. After the Na_2SO_4 was removed by filtration, the solvent was removed under reduced pressure to obtain DA-EG2 as a colorless oil (6.75 g, 99 %). ^{1}H NMR (400 MHz, 298 K, $CDCl_3$): δ 3.69 (t, J = 9.5 Hz, 4H), 3.68 (s, 4H), 3.40 (t, J = 9.5 Hz, 4H).

Preparation of (*Z*)-1,4-Bis(prop-2-yn-1-yloxy)but-2-ene (DY).[17] A solution of *cis*-butene-1,4-diol (15.2 g, 172 mmol) in THF (80 mL) was added dropwise to a suspension of sodium hydride (27.9 g, 698 mmol, 60% suspension in paraffin liquid) in THF (400 mL) under a nitrogen atmosphere in an ice-water bath. The mixture was stirred at room temperature for 15 min, and then propargyl bromide (48 mL, 442 mmol, 80% in toluene) was added. After stirring at room temperature overnight, THF was removed under reduced pressure. To the residue, water (150 mL) was added slowly. The product was extracted with dichloromethane (3 × 100 mL). The organic layers were combined. The combined organic phase was washed with water (50 mL) and dried over Na_2SO_4. After the Na_2SO_4 was removed by filtration, the solvent was removed under reduced pressure to obtain a brown oil (40.5 g). The product was purified by distillation under reduced pressure to obtain a colorless oil (26.3 g, 161 mmol, 93 %). Bp: 55 °C / 0.17

mmHg. ^{1}H NMR (500 MHz, 298 K, $CDCl_3$): δ 5.76 (ddd, J = 4.9, 3.8, and 1.2 Hz, 2H), 4.16 (dd, J = 3.8 and 1.2 Hz, 4H), 4.16 (d, J = 2.5 Hz, 4H), 2.44 (t, J = 2.5 Hz, 2H).

Preparation of Monotosylate of Triethylene Glycol (MTs-EG2).[18] Triethylene glycol (58.5 g, 390 mmol) and triethylamine (10.5 mL, 75.8 mmol) were dissolved in dichloromethane (30 mL). *p*-Toluenesulfonyl chloride (9.81 g, 51.6 mmol) was added slowly to the solution cooled with an ice-water bath. After stirring for 18 h at room temperature, the reaction mixture was diluted with dichloromethane (50 mL). The resulting solution was washed with 5% citric acid (2 × 50 mL) and saturated aqueous NaCl (100 mL). The solution was dried over Na_2SO_4 and the Na_2SO_4 was removed by filtration. The solvent was removed under reduced pressure to obtain a yellow oil (14.6 g). The product was purified by column chromatography using ethyl acetate to obtain a colorless oil (13.2 g, 84 %). ^{1}H NMR (500 MHz, 298 K, $CDCl_3$): δ 7.81 (d, J = 8.0 Hz, 2H), 7.35 (d, J = 8.0 Hz, 2H), 4.17 (t, J = 4.8 Hz, 2H), 3.72 (t, J = 4.8 Hz, 2H), 3.71 (t, J = 4.8 Hz, 2H), 3.61 (s, 4H), 3.66 (t, J = 4.8 Hz, 2H), 2.45 (s, 3H).

Preparation of Monoazide of Triethylene Glycol (MA-EG2).[16] MTs-EG2 (30.4 g, 99.8 mmol) was dissolved in DMSO (100 mL). To the solution, sodium azide (10.4 g, 160 mmol) was added. After stirring at room temperature overnight, saturated aqueous NaCl (100 mL) was added to the reaction mixture. The product was extracted

with diethyl ether (3 × 200 mL). The organic layers were combined. The combined organic phase was washed with saturated aqueous NaCl (20 mL) and then dried over $MgSO_4$. The $MgSO_4$ was removed by filtration. The solvent was removed under reduced pressure to obtain MA-EG2 as a colorless oil (13.5 g, 65 %). ^{1}H NMR (500 MHz, 298 K, $CDCl_3$): δ 3.77–3.69 (m, 2H), 3.68–3.66 (m, 6H), 3.62 (t, J = 4.8 Hz, 2H), 3.41 (t, J = 4.8 Hz, 2H).

Synthesis of 1,2-Bis(2-(4-((((*Z*)-4-(prop-2-yn-1-yloxy)but-2-en-1-yl)oxy)methyl)-1H-1,2,3-triazol-1-yl)ethoxy)ethane (1).[19] A solution of DA-EG2 (622 mg, 3.12 mmol) in THF (50 mL) was added dropwise to a mixture of DY (4.92 g, 30.0 mmol), CuBr (20 mg, 0.15 mmol), and PMDETA (33 μL, 0.15 mmol) in THF (5 mL) with cooling by an ice-water bath. After stirring for 8 h under a nitrogen atmosphere, the solvent was removed under reduced pressure. To the residue, chloroform (100 mL) was added, and the solution was washed with aqueous EDTA·4Na (0.5 M, 100 mL) and water (3 × 100 mL). The organic phase was dried over Na_2SO_4. After the Na_2SO_4 was removed by filtration, the solvent was removed under reduced pressure to obtain a pale brown oil (5.34 g). The oil was fractionated by column chromatography using a mixed solvent of hexane, ethyl acetate, and methanol (20/1/0 – 0/20/1, v/v/v) to obtain **1** as a pale yellow oil (1.19 g, 72 %). ^{1}H NMR (400 MHz, 298 K, $CDCl_3$): δ 7.69 (s, 2H), 5.82–5.67 (m, 4H),

4.63 (s, 4H), 4.52 (t, J = 10.4 Hz, 4H), 4.20–4.12 (m, 12H), 3.83 (t, J = 10.4 Hz, 4H), 3.56 (s, 4H), 2.45 (t, J = 2.5 Hz, 2H). HRMS (ESI) m/z: $[M + Na]^+$ calcd for $C_{26}H_{35}N_6NaO_6$ 551.2594; found 551.2606.

Synthesis of a Hydroxy-Terminated Linear Dimer (2).[19] A solution of MA-EG2 (357 mg, 2.04 mmol) in THF (100 mL) was added dropwise to a mixture of **1** (5.34 g, 10.1 mmol), CuBr (27 mg, 0.19 mmol), and PMDETA (42 μL, 0.20 mmol) in THF (5 mL) with cooling by an ice-water bath over 30 min. After stirring overnight at room temperature under a nitrogen atmosphere, the solvent was removed under reduced pressure to obtain a brown oil. The oil was fractionated by column chromatography using a mixed solvent of ethyl acetate and methanol (20/1 – 3/1, v/v) to obtain **2** as an orange oil (1.01 g, 71 %). ^{1}H NMR (500 MHz, 298 K, $CDCl_3$): δ 7.81 (s, 1H), 7.70 (s, 1H), 7.69 (s, 1H), 5.80–5.69 (m, 4H), 4.64–4.60 (m, 6H), 4.60–4.49 (m, 6H), 4.19–4.10 (m, 10H), 3.88 (t, J = 5.0 Hz, 2H), 3.83 (q, J = 4.5 Hz, 4H), 3.72 (t, J = 4.5 Hz, 2H), 3.62 (s, 4H), 3.58–3.54 (m, 6H), 2.45 (t, J = 2.3 Hz, 1H). HRMS (ESI) m/z: $[M + Na]^+$ calcd for $C_{32}H_{49}N_9NaO_9$ 726.3551; found 726.3545.

Synthesis of a Linear Dimer (*l*-ene2).[20] DIAD (420 μL, 2.17 mmol) was added to a solution of triphenylphosphine (559 mg, 2.13 mmol) in THF (6 mL) with cooling by an ice-water bath. After stirring for 10 min, DPPA (460 μL, 2.13 mmol) was added

dropwise at room temperature. To the resulting mixture, a solution of **2** (1.00 g, 1.42 mmol) in THF (4 mL) was added. After stirring for 24 h, the solution was heated at 40 °C for 17 h. The mixture was heated at 60 °C for 24 h and the solvent was removed under reduce pressure to obtain a yellow oil. The oil was fractionated by column chromatography using a mixed solvent of ethyl acetate and methanol (1/0 – 3/1) to obtain *l*-ene2 as a yellow oil (459 mg, 44%). ^{1}H NMR (500 MHz, 298 K, $CDCl_3$): δ 7.74 (s, 1H), 7.70 (s, 1H), 7.69 (s, 1H), 5.80–5.67 (m, 4H), 4.64–4.58 (m, 6H), 4.56–4.47 (m, 6H), 4.19–4.10 (m, 10H), 3.89 (t, J = 5.0 Hz, 2H), 3.65 (m, 6H), 3.58–3.53 (m, 6H), 3.37 (t, J = 5.0 Hz, 2H), 2.45 (t, J = 2.3 Hz, 1H). HRMS (ESI) m/z: $[M + Na]^+$ calcd for $C_{32}H_{48}N_{12}NaO_8$ 751.3606; found 751.3607.

Synthesis of a Cyclic Dimer (*c*-ene2).[21] A solution of *l*-ene2 (145 mg, 0.19 mmol) in methanol (50 mL) was added dropwise using a syringe pump at a rate of 7.2 mL h^{-1} to a mixture of CuBr (1.42 g, 9.96 mmol) and PMDETA (2.10 mL, 10.1 mmol) in methanol (50 mL) at room temperature. After stirring for 60 h, water (100 mL) was added to the mixture, and the product was extracted with dichloromethane (3 × 50 mL). The organic layers were combined. The combined organic phase was washed with water (3 × 30 mL) and dried over Na_2SO_4. After the Na_2SO_4 was removed by filtration, the solvent was removed under reduced pressure to obtain a brown oil (146 mg). The oil was

fractionated by column chromatography using a mixed solvent of ethyl acetate and methanol (1/1, v/v) to obtain *c*-ene2 as a colorless solid (72 mg, 50 %). ^{1}H NMR (500 MHz, 298 K, $CDCl_3$): δ 7.73 (s, 4H), 5.76–5.67 (m, 4H), 4.59 (s, 8H), 4.51 (t, J = 10.5 Hz, 8H), 4.10 (d, J = 4.5 Hz, 8H), 3.81 (t, J = 10.5 Hz, 8H), 3.55 (s, 8H). HRMS (ESI) m/z: $[M + Na]^+$ calcd for $C_{32}H_{48}N_{12}NaO_8$ 751.3606; found 751.3605.

Synthesis of a Cyclic Dimer Bearing Adamantyl Moieties (*c*-Ad2).[22] 1-Adamantanethiol (77 mg, 0.46 mmol), *c*-ene2 (31 mg, 0.042 mmol), and DMPA (24 mg, 0.093 mmol) were dissolved in DMF (1.5 mL). The solution was irradiated with 365 nm UV light for 6 h. The reaction mixture was added dropwise to diethyl ether (30 mL). A viscous oil was recovered by centrifugation at 4,000 rpm for 15 min followed by decantation to obtain *c*-Ad2 as a yellow oil (23 mg, 51 %). ^{1}H NMR (400 MHz, 298 K, $CDCl_3$): δ 7.87–7.58 (br, 4H), 4.68–4.23 (br, 16H), 3.89–3.67 (br, 8H), 3.61–3.36 (br, 8H), 2.14–1.43 (br, 30H). HRMS (ESI) m/z: $[M + Na]^+$ calcd for $C_{52}H_{80}N_{12}NaO_8S_2$ 1087.5561; found 1087.5524.

Synthesis of a Cyclic Dimer Bearing Carboxy Moieties (*c*-C2).[22] Mercaptacetic acid (300 μL, 5.73 mmol), *c*-ene2 (287 mg, 0.40 mmol), and DMPA (51 mg, 0.20 mmol) were dissolved in DMF (3.0 mL). After deoxygenation by purging with nitrogen for 10 min, the solution was irradiated with 365 nm UV for 12 h. To the reaction

solution, water (20 mL) was added. The mixture was washed with diethyl ether (3 × 10 mL). The solvent was removed under reduced pressure. The residue was dissolved in methanol (2 mL). The solution was added dropwise to diethyl ether (40 mL). A viscous oil was recovered by centrifugation at 4,000 rpm for 15 min followed by decantation to obtain *c*-C2 as a yellow oil (350 mg, 95 %). ^{1}H NMR (500 MHz, 298 K, D_2O): δ 7.96–7.84 (m, 4H), 4.59–4.40 (m, 16H), 3.84–3.72 (m, 8H), 3.65–3.37 (m, 16H), 3.30–3.15 (m, 4H), 2.95–2.87 (br, 2H), 1.86–1.74 (m, 2H), 1.64–1.53 (m, 2H). HRMS (ESI) *m*/*z*: [M + Na]$^+$ calcd for $C_{36}H_{57}N_{12}O_{12}S_2$ 913.3660; found 913.3660.

Synthesis of a Cyclic Dimer Bearing βCD Moieties (*c*-βCD2).[23] *c*-C2 (250 mg, 0.7 mmol), DCC (155 mg, 0.75 mmol), and HOBt (97 mg, 0.72 mmol) were dissolved in DMF (10 mL). To the solution, NH_2-βCD (841 mg, 0.74 mmol) was added. After stirring for 90 h at room temperature, the mixture was added dropwise to acetone (200 mL) to obtain pale brown solid (1.04 g). The product was purified by preparative TLC using a mixed solvent of 1-butanol, ethanol, and water (1/1/2, v/v/v) containing 0.5% triethylamine. The silica gel particles on which the product was adsorbed were collected. The product was extracted from the silica gel using DMF. The solution was concentrated and added to a large excess of acetone to obtain *c*-βCD2 as a pale brown solid (124 mg, 6 %). ^{1}H NMR (500 MHz, 298 K, D_2O): δ 7.98–7.80 (m, 4H), 5.13–4.99 (m, 14H), 4.58–

4.49 (m, 16H), 4.09–3.30 (m, 108H), 3.30–3.15 (m, 4H), 2.95–2.87 (br, 2H), 1.86–1.74 (m, 2H), 1.64–1.53 (m, 2H). HRMS (MALDI) *m*/*z*: $[M + Na]^+$ calcd for $C_{120}H_{194}N_{14}NaO_{78}S_2$ 3166.0983; found 3166.0804.

3-3. Results and Discussion

Synthesis of a Cyclic Dimer (*c*-ene2). To synthesize multivalent molecules, a cyclic dimer (*c*-ene2), onto which interaction moieties can be introduced, was designed and synthesized in this study. First, according to Scheme 3-1, triethylene glycol with azide moieties at both ends (DA-EG2) was prepared by azidation of the ditosylate using sodium azide. Dialkyne (DY) was obtained by coupling of a diol possessing an internal alkene with propargyl bromide under basic conditions (Scheme 3-2). Compound **1** was synthesized from DA-EG2 and DY through CuAAC catalyzed by a CuBr/PMDETA system using a large excess of DY. Hydroxy-terminated linear dimer **2** was obtained by CuAAC coupling of **1** and monoazide of triethylene glycol (MA-EG2). After azidation of **2** using diphenylphosphoryl azide (DPPA), *c*-ene2 was synthesized through intramolecular cyclization by CuAAC. The selective cyclization was achieved by slowly dropping a dilute solution of the linear dimer (*l*-ene2) into a solution of CuBr/PMDETA. The products were characterized by ^{1}H NMR and MS (see Figure 3-1 and Experimental

Section). Figure 3-1 displays a typical example of ^{1}H NMR spectra for **1**, **2**, *l*-ene2, and *c*-ene2. All the spectra contain signals ascribable to the protons of triazole and internal alkene at 7.8 and 5.7 ppm, respectively. These spectra also contain signals due to the methylene protons at 3.5–4.6 ppm. In the spectrum for **2** (Figure 3-1B), signals ascribable to the methylene attached to the hydroxy group appear at 3.7 ppm. On the other hand, Figure 3-1C shows signals assignable to the methylene protons attached to the azide group are seen at 3.4 ppm. There are no signals ascribable to the methylene and methine protons of the terminal propargyl group at 3.4 and 2.5 ppm in the spectrum for *c*-ene2 (Figure 3-1D). These data indicate that *c*-ene2 was successfully synthesized.

Scheme 3-1. Preparation of DA-EG2 (A) and DY (B)

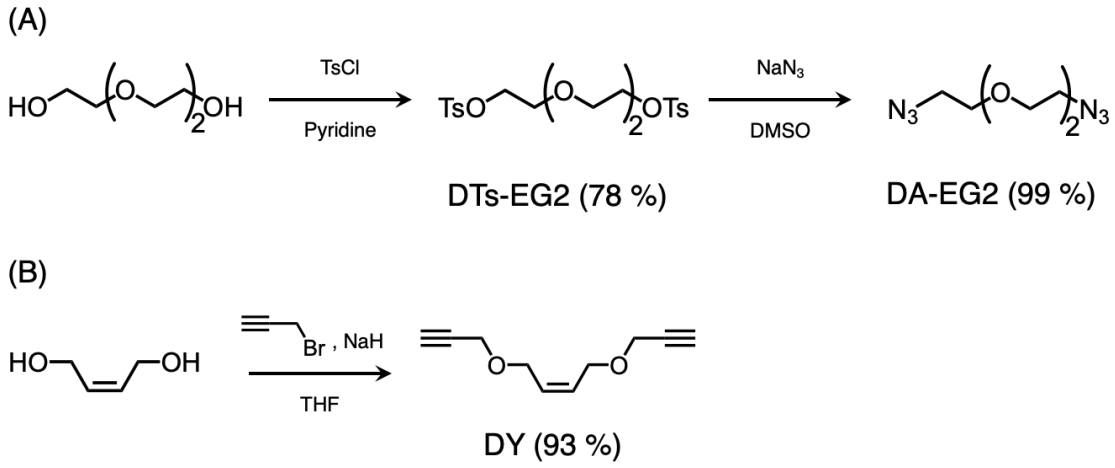

Scheme 3-2. Synthesis of *c*-ene2

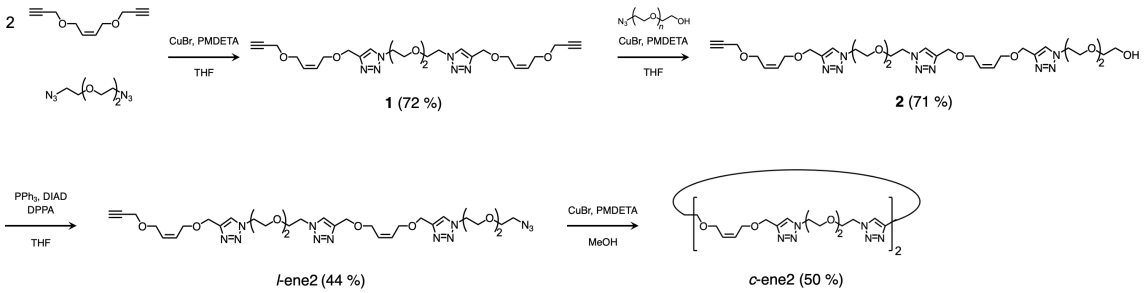

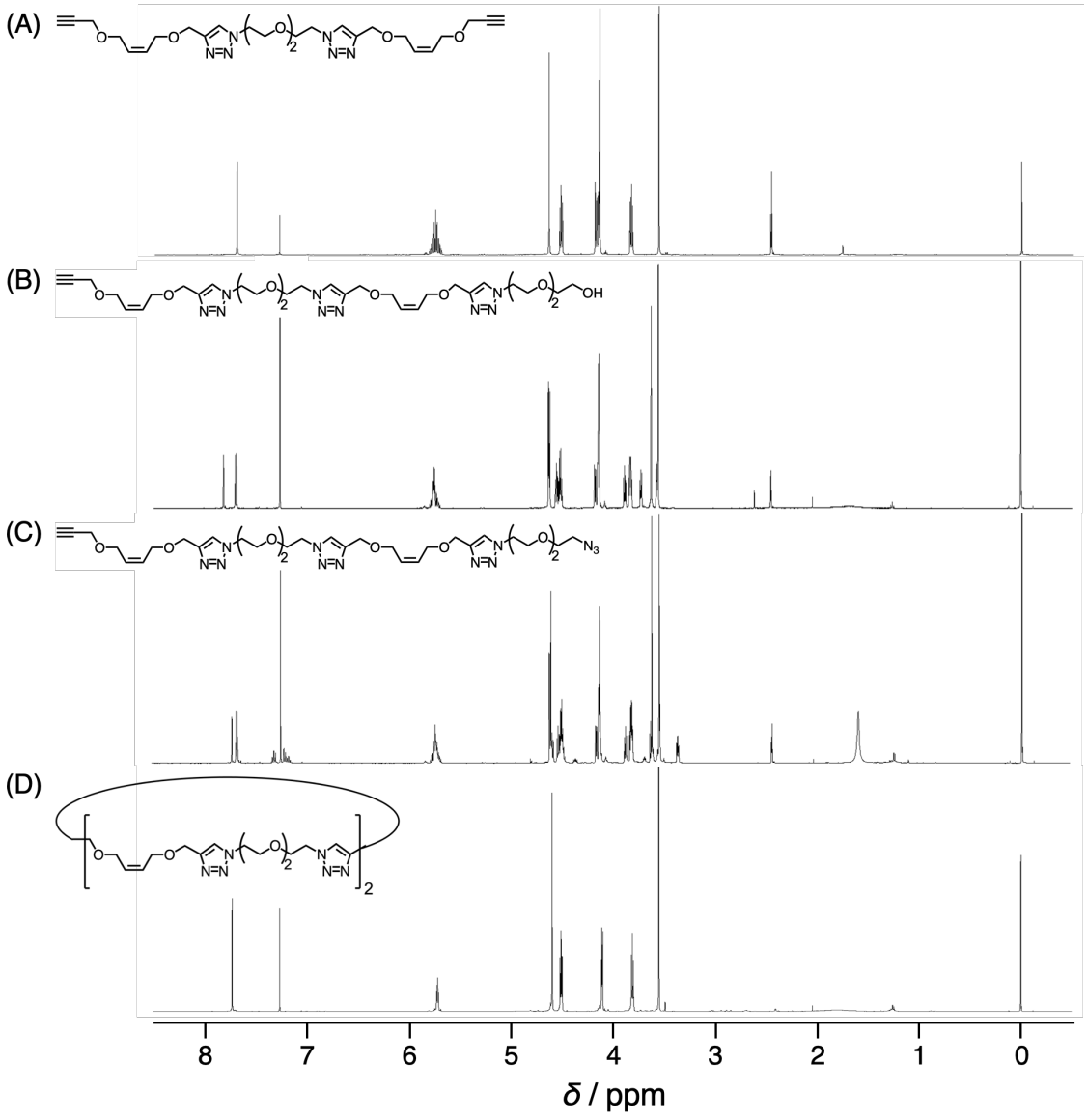

Figure 3-1. ^{1}H NMR spectra for **1** (A), **2** (B), *l*-ene2 (C), and *c*-ene2 (D) in $CDCl_3$.

Introduction of Ad and βCD moieties to *c*-ene2. Aiming at study on the interaction of multivalent molecules (Chapter 4), interaction sites were introduced to *c*-ene2. A pair of Ad and βCD moieties have been chosen as interacting cites in this study, because Ad and βCD moieties form rather stable inclusion complexes in water (association constant $K_a \sim 10^{-4}$ M).[24] A cyclic guest dimer bearing Ad moieties (*c*-Ad2) was synthesized by thiol–ene reaction using DMPA as a photoinitiator according to Scheme 3-3. The complementary dimer (*c*-βCD2) was prepared in two steps as can be seen in Scheme 3-4; *c*-C2 was obtained by thiol-ene reaction using thioglycolic acid, followed by coupling with NH_2-βCD to synthesize *c*-βCD2. The products were characterized by ^{1}H NMR and MS (see Figure 3-2 and Experimental Section). Figure 3-2 displays ^{1}H NMR spectra for *c*-ene2, *c*-Ad2, *c*-C2, and *c*-βCD2 in D_2O. All the spectra contain signals ascribable to the triazole proton at 7.8 ppm. In the spectrum for *c*-Ad2 (Figure 3-2B), signals due to the internal alkene at ca. 5.7 ppm are not seen. There are signals assignable to the methine and methylene protons in adamantyl moieties in the region of 1.5–2.0 ppm. All signals due to *c*-Ad2 are broad presumably because of the limited solubility in D_2O. Figure 3-2C shows signals ascribable to the methylene protons next to the carbonyl carbon at 3.2 ppm instead of signals due to the internal alkene. There are signals due to βCD in the region of 3.4–4.0 ppm in the spectrum for *c*-βCD2 (Figure

3-2D). These data are indicative of successful synthesis of *c*-Ad2 and *c*-βCD2.

Scheme 3-3. Synthesis of *c*-Ad2

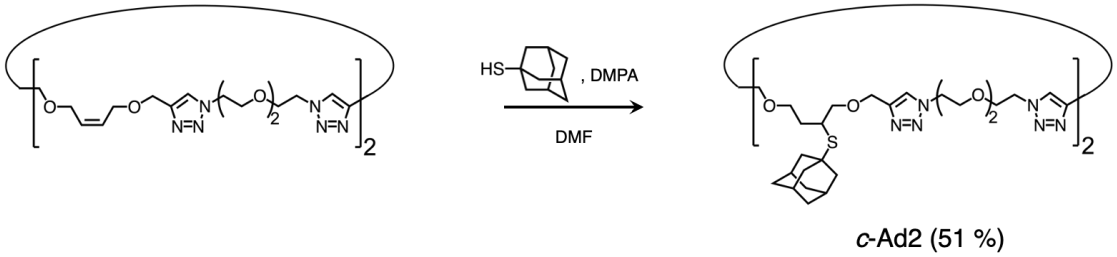

Scheme 3-4. Synthesis of *c*-βCD2

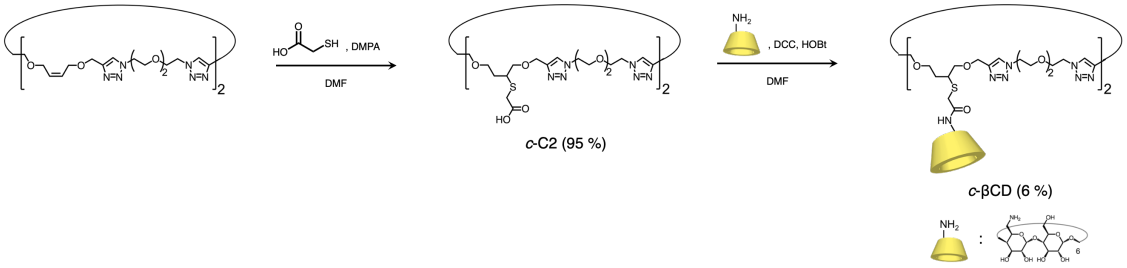

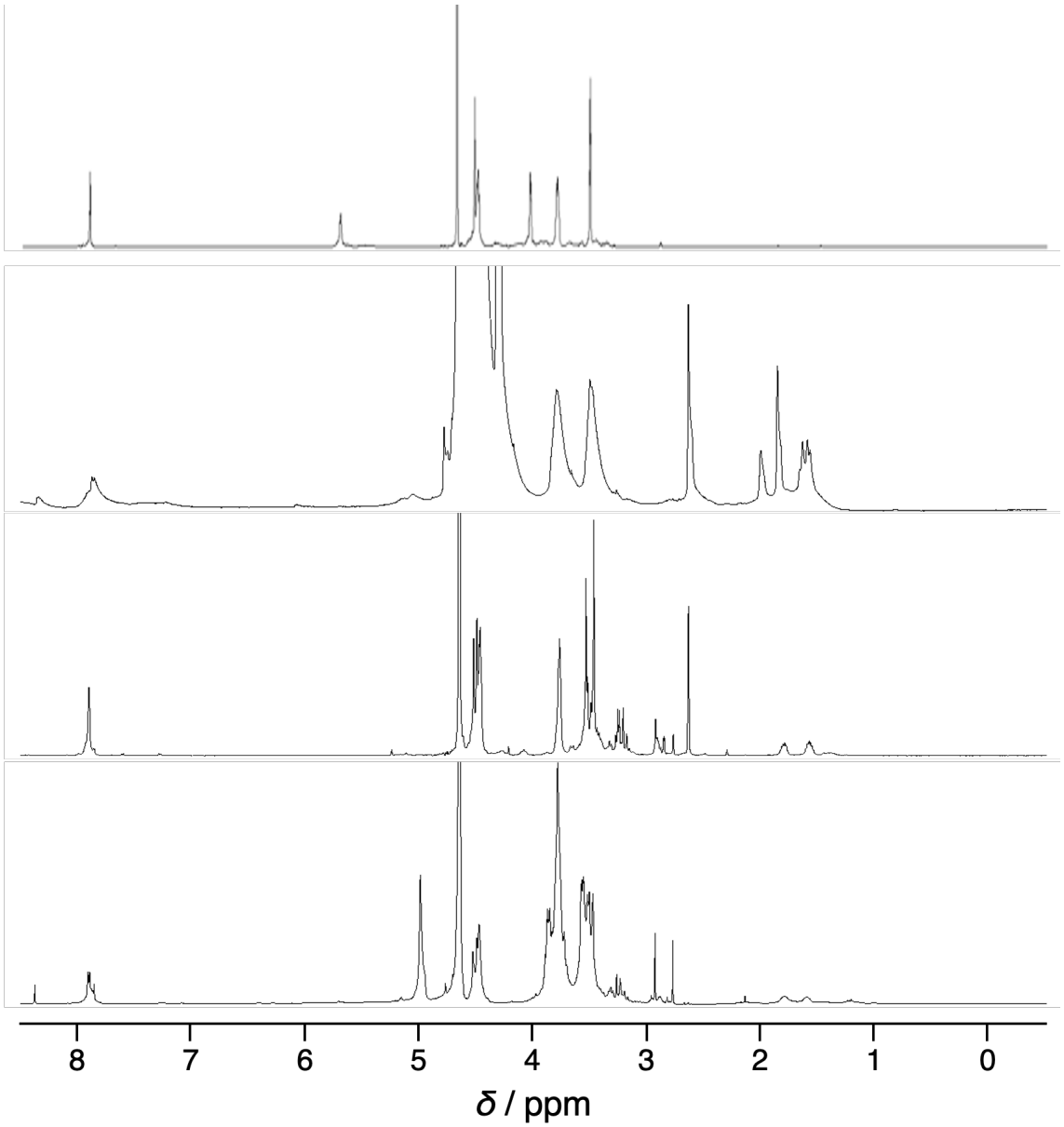

Figure 3-2. ^{1}H NMR spectra for *c*-ene (A), *c*-Ad2 (B), *c*-C2 (C), and *c*-βCD2 (D) in D_2O.

3-4. Conclusions

In this study, the author synthesized cyclic host and guest dimers in order to study on the multivalency in detail. First, linear dimer (*l*-ene2) was synthesized by stepwise

CuAAC of diazide formed from triethylene glycol and dialkyne possessing internal alkene. A cyclic dimer (*c*-ene2) was obtained by selective intramolecular cyclization through CuAAC under highly diluted conditions. Cyclic dimers bearing βCD and Ad moieties were synthesized by thiol–ene and amide coupling reactions.

3-5. References

(1) Pedersen C. J. *J. Am. Chem. Soc.* **1967**, *89*, 2495–2496.

(2) Szejtli, J. *Chem. Rev.* **1998**, *98*, 1743–1753.

(3) Gutsche, C. D.; Dhawan, B.; No, K. H.; Muthukrishnan, R. *J. Am. Chem. Soc.* **1981**, *103*, 3782–3792.

(4) Del Valle, E. M. M. *Process Biochem.* **2004**, *39*, 1033–1046.

(5) Yoo, C.; Dodge H. M.; Miller, A. J. M. *Chem. Commun*. **2019**, *55*, 5047–5059.

(6) Ma, X.; Zhao, Y. *Chem. Rev.* **2015**, *115*, 7794–7839.

(7) Goto, Y.; Ohta, A.; Sako, Y.; Yamagishi, Y.; Murakami, H.; Suga, H. *ACS Chem. Biol.* **2008**, *3*, 120–129.

(8) Zorzi, A.; Deyle, K.; Heinis, C. *Curr. Opin. Chem. Biol.* **2017**, *38*, 24–29.

(9) Kolb, H. C.; Finn, M. G.; Sharpless, K. B. *Angew. Chem. Int. Ed.* **2001**, *40*, 2004–2021.

(10) Rostovtsev, V. V.; Green, L. G.; Fokin, V. V.; Sharpless, K. B. *Angew. Chem. Int. Ed.* **2002**, *41*, 2596–2599.

(11) Tornøe, C. W.; Christensen, C.; Meldal, M. *J. Org. Chem.* **2002**, *67*, 3057–3064.

(12) Posner, T. *Chem. Ber.* **1905**, *38*, 646–657.

(13) Hurd, C. D.; Gershbein, L. L. *J. Am. Chem. Soc.* **1947**, *69*, 2328–2335.

(14) Binauld, S.; Hawker, C. J.; Fleury, E.; Drockenmuller, E. *Angew. Chem. Int. Ed.* **2009**, *48*, 6654 –6658.

(15) Gunsow, O. A.; Kausar, A. R.; Triplett, K. B. *J. Heterocyclic Chem.* **1981**, *18*, 297–302.

(16) Sandmann, B.; Happ, B.; Hager, M. D.; Vitz, J.; Rettler, E.; Burtscher, P.; Moszner, N.; Schubert, U. S. *J. Polym. Sci., A, Polym. Chem.* **2014**, *52*, 239–247.

(17) Iafe, R. G.; Kuo, J. L.; Hochstatter, D. G.; Saga, T.; Turner, J. W.; Merlic, C. A. *Org. Lett.* **2013**, *15*, 582–585.

(18) van Ameijde, J.; Liskamp, R. M. J. *Org. Biomol. Chem.* **2003**, *1*, 2661–2669.

(19) Berthet, M.-A.; Zarafshani, Z.; Pfeifer, S.; Lutz, J.-F. *Macromolecules* **2010**, *43*, 44–50.

(20) Comstock, L. R.; Rajski, S. R. *Tetrahedron* **2002**, *58*, 6019–6026.

(21) Lonsdale, D. E.; Bell, C. A.; Monteiro, M. J. *Macromolecules* **2010**, *43*, 3331–3339.

(22) Killops, K. L.; Campos, L. M.; Hawker, C. J. *J. Am. Chem. Soc.* **2008**, *130*, 5062–5064.

(23) Ogoshi, T.; Takashima, Y.; Yamaguchi, H.; Harada, A. *J. Am. Chem. Soc.* **2007**, *129*, 4878–4879.

(24) Rekharsky, M. V.; Inoue Y. *Chem Rev.* **1998**, *98*, 1875–1917.

Chapter 4

Interaction of Interval-Controlled Cyclic Dimers Synthesized by Click Chemistry

4-1. Introduction

Recently, multivalency has been recognized to play an important role in the molecular recognition of biomolecules for biological activities.[1,2] Inspired by the multivalency in nature, stable and reversible systems based on multiple weak non-covalent bondings of synthetic polymers are used in a wide range of fields, e.g., drug delivery systems,[3–5] self-healing materials,[6–8] and stimuli-responsive materials.[9–10] Detailed studies on multivalency are necessary for understanding the specific molecular recognition systems of biomolecules and for designing new functional polymeric materials based on molecular recognition. However, multivalent polymers synthesized by general polymerization techniques have considerable distributions of their structures, e.g, monomer sequence and molecular weight, making it difficult to investigate multivalency in detail. Therefore, investigating the interactions of multivalent molecules with well-defined structures plays an important role in relating the molecular structure to the multivalency.

The author focuses on the interactions of interval-controlled cyclic dimers, one

of the simplest multivalent molecules. In this chapter, interval-controlled cyclic dimers bearing β-cyclodextrin (βCD) and adamantyl (Ad) moieties synthesized in Chapter 3 are used. To investigate the association behavior of the interval-controlled cyclic host dimer (*c*-βCD2), firstly, the author focuses on the polymer/dimer interaction system and investigates the interactions of poly(acrylic acid) bearing naphthyl (Np) residues of different contents with the interval-controlled cyclic host dimer by fluorescence measurements. Next, focusing on the dimer/dimer interaction system, the interactions of the interval-controlled cyclic guest dimer (*c*-Ad2), i.e., the counterpart of *c*-βCD2, with several host molecules are investigated by NMR techniques.

4-2. Experimental Section

Materials. Tris[2-(dimethylamino)ethyl]amine (Me_6TREN) and *t*-butyl 2-bromoisobutyrate (*t*BuB) were purchased from Tokyo Chemical Industry Co., Ltd. (Tokyo, Japan). *N*,*N*′-Dicyclohexylcarbodiimide (DCC), 1-hydroxybenzotriazole (HOBt), anhydrous sodium sulfate (Na_2SO_4), tetra-sodium ethylenediaminetetraacetate (EDTA·4Na), *N*,*N*-dimethylformamide (DMF), and dichloromethane were purchased from Nacalai Tesque Inc. (Kyoto, Japan). Copper (powder), 2-naphthylmethylamine, *t*-butyl acrylate (*t*BuA), trifluoroacetic acid (TFA), diethyl ether, ethyl acetate, hexane,

methanol, and toluene were purchased from FUJIFILM Wako Pure Chemical Corp. (Osaka, Japan). Water was purified with a Millipore Milli-Q system. Other reagents were used as received.

Measurements. ^{1}H NMR spectra were recorded on a JEOL JNM ECS400 or ECA500 spectrometer using deuterium oxide (D_2O) as a solvent. Pulse-field-gradient spin-echo (PGSE) NMR data were obtained on a Bruker Advance 700 NMR spectrometer. The bipolar pulse pair stimulated echo (BPPSTE) sequence was applied.[13–15] The strength of pulsed gradients (g) was increased from 0.3 to 90 gauss cm^{-1}. The time separation of pulsed field gradients (Δ) and their duration (δ) were 0.15 and 0.002 s, respectively. The sample was not spun and the airflow was disconnected. The shape of the gradient pulse was rectangular, and its strength was varied automatically during the course of the experiments. Two-dimensional diffusion ordered spectroscopy (2D DOSY) data were obtained by inverse Laplace transformation using the SPLMOD method.[16,17] Fluorescence measurements were performed on a SHIMADZU RF-5300PC equipped with a single cuvette reader at room temperature. The slit widths for both the excitation and emission sides were kept at 5.0 nm during measurement.

Preparation of Poly(*t*BuA).[18] Copper (powder, 332 mg, 5.18 mmol) was added to a schlenk flask. The flask was degassed and backfilled with nitrogen three times. *t*BuA

(40.0 mL, 275 mmol), *t*BuB (1.00 mL, 5.40 mmol), Me_6TREN (1.40 mL, 5.20 mmol), and toluene (20 mL) were added to the flask. After bubbling with nitrogen for 10 min, the solution was stirred at room temperature for 24 h. The reaction mixture was diluted with ethyl acetate (300 mL). The resulting solution was washed with aqueous EDTA·4Na (0.5 M, 3 × 50 mL) and dried over Na_2SO_4. After filtration, the solvent was removed under reduced pressure. The product was purified by reprecipitation twice using a mixed solvent of diethyl ether, methanol, water (1/5/5, v/v/v) to obtain poly(*t*BuA) as a pale yellow solid (34.3 g, 94 %).

Preparation of Poly(acrylic acid) (poly(AA)).[19] TFA (80 mL, 1.04 mol) was added to a solution of poly(*t*BuA) (34.1 g, 266 mmol of *t*-butyl ester) in dichloromethane (80 mL). After stirring at room temperature overnight, the mixture was poured into hexane (500 mL) to form a precipitate. After decantation, the precipitate was washed with hexane (2 × 200 mL). The product was dried under reduced pressure to obtain poly(AA) as a colorless solid (23.6 g, 88 %).

Preparation of Poly(AA) Bearing Np Moieties (p(AANa/Np*x*)).[20] A typical procedure is described below.

A solution of DCC (481 mg, 2.33 mmol) in DMF (5 mL) was added to a solution of poly(AA) (937 mg, 13 mmol monomer units) in DMF (10 mL) in ice-water bath. To

the mixture, HOBt (312 mg, 2.31 mmol) was added. A solution of 2-naphthylmethylamine (407 mg, 2.59 mmol) in DMF (5 mL) was added to the reaction mixture. The mixture was stirred for 48 h at room temperature. After filtration, the solvent was removed under reduced pressure. The product was purified by reprecipitation twice from DMF into ethyl acetate to obtain a pale yellow solid (2.02 g, 75 %). The degree of modification was determined to be 14.7 mol% by ^{1}H NMR.

4-3. Results

Interaction of p(AANa/Np*x*) with βCD and *c*-βCD2. To investigate the binding behavior of the interval-controlled cyclic host dimer, the author has started the study with the polymer/dimer interaction systems, in which Np moiety has been employed for fluorescence measurements. Thus, poly(acrylic acid)s bearing Np moieties (p(AANa/Np*x*), where *x* is the mol% content of Np groups) were used as guest polymers (Figure 4-1). Fluorescence spectra of aqueous solutions of p(AANa/Np6) and p(AANa/Np15) were measured in the absence and presence of varying concentrations of βCD or *c*-βCD2 (Figure 4-2). In all the spectra, signals due to monomer emission of Np moieties are observed at ca. 340 nm. In the case of βCD, the signal intensity increases with βCD concentration, indicative of the formation of one-to-one complexes. On the

other hand, in the case of *c*-βCD2, the signal intensity increases with βCD concentration and then decreases at higher concentrations, indicative of the formation of higher-order complexes rather than one-to-one complexes. The ratios of signal intensities at 334 nm in the presence and absence of βCD (I/I_0) were calculated and plotted in Figure 4-3 against βCD concentration. The analysis of data will be described in the following subsection.

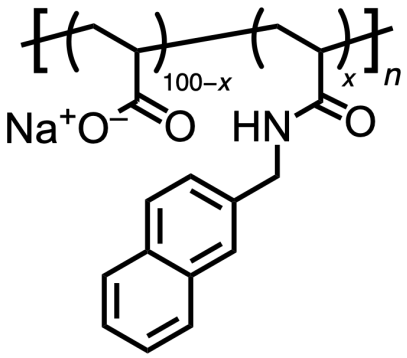

p(AANa/Np*x*)

Figure 4-1. Chemical structure of p(AANa/Np*x*).

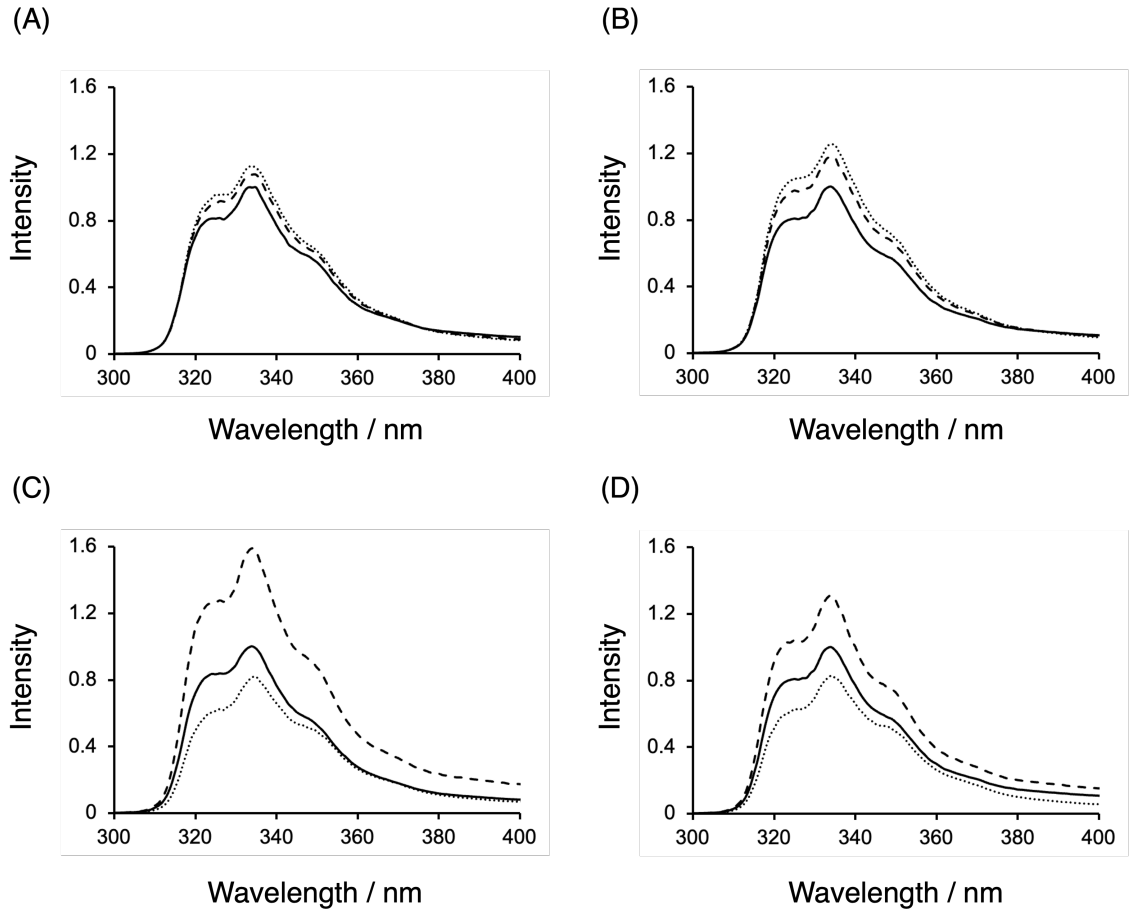

Figure 4-2. Fluorescence spectra of aqueous p(AANa/Np6) (A) and p(AANa/Np15) (B) in the absence (solid line) and presence of 0.13 mM (broken line) and 0.25 mM βCD (dotted line), and aqueous p(AANa/Np6) (C) and p(AANa/Np15) (D) in the absence (solid line) and presence of 0.07 mM (broken line) and 0.11 mM *c*-βCD2 (dotted line).

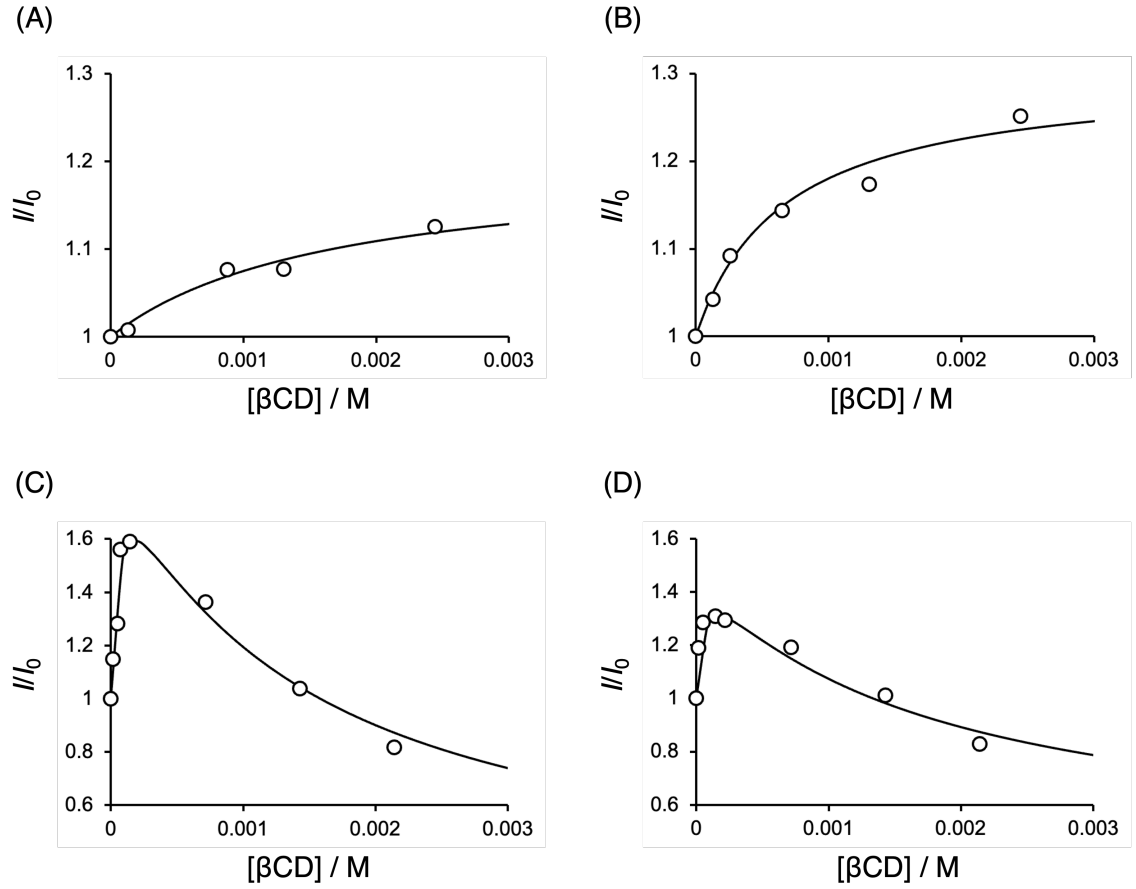

Figure 4-3. Plots of I/I_0 against βCD concentration for aqueous p(AANa/Np6) (A) and p(AANa/Np15) (B) with βCD with a best-fit curve using eq 4-7, and aqueous p(AANa/Np6) (C) and p(AANa/Np15) (D) with *c*-βCD2 with a best-fit curve using eq 4-15.

Interaction of *c*-Ad2 with Host Molecules. The author also focused on the interaction of the complementary guest dimer (*c*-Ad2). *c*-Ad2 exhibited a limited solubility in water presumably because of the hydrophobicity of Ad moieties; *c*-Ad2 (2 mg) did not dissolved completely in water (1 mL). On the other hand, *c*-Ad2 (2 mg) was

completely soluble in 10 mM βCD solution (1 mL), indicating that βCD solubilized *c*-Ad2 by the formation of inclusion complexes between the Ad moieties and βCD. As can be seen in Figure 4-4, the ROESY for a D_2O solution containing *c*-Ad2 and βCD shows the correlation signals between the signals ascribable to the Ad moieties (2.2–1.7 ppm) and the signals due to the βCD inner protons (ca. 3.7 and 3.8 ppm). This observation confirmed the formation of inclusion complexes between the Ad moieties and βCD.

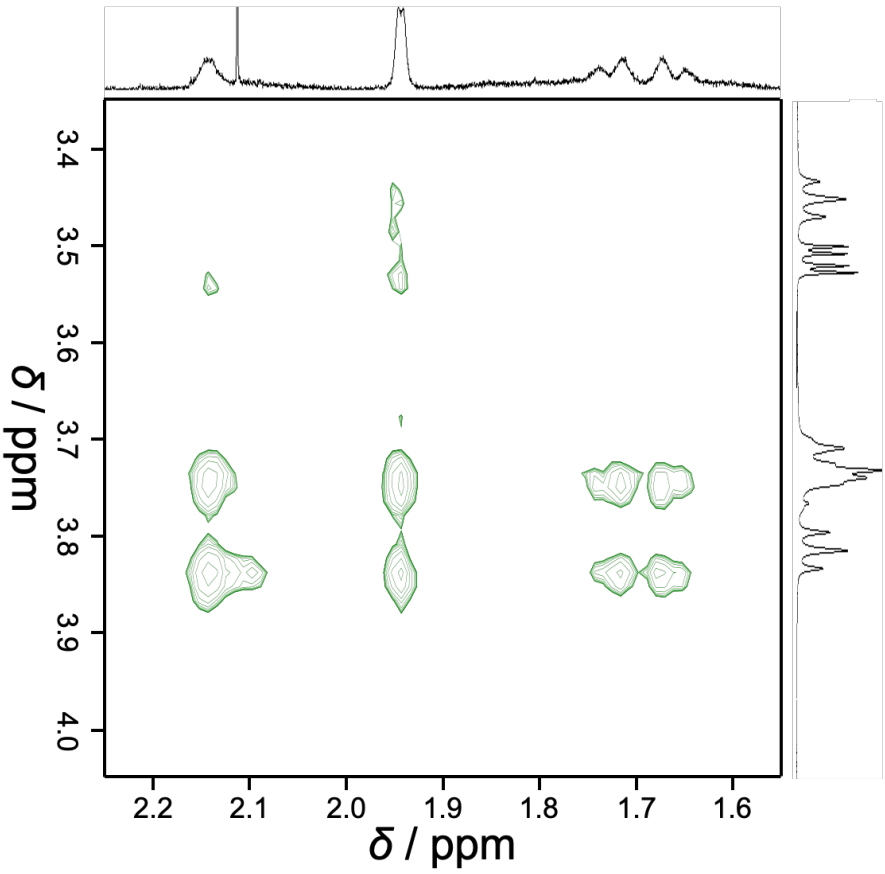

Figure 4-4. ROESY for a solution of *c*-Ad2 in 10 mM D_2O of βCD.

The interactions of *c*-Ad2 with host molecules, i.e., βCD, βCD2-1, βCD2-2 (Figure 4-5), and *c*-βCD2, were investigated by ^{1}H NMR measured at varying concentrations of the host molecules (Figure 4-6). In all the cases, the signals due to the Ad moieties shift to lower magnetic fields with increasing the host concentration. The differences in the chemical shifts in the presence and absence of the host molecules ($\Delta\delta$) were calculated and plotted in Figure 4-7 against the concentration of βCD moiety ([βCD]). These data in Figure 4-7 indicate that the interactions of *c*-Ad2 with βCD and βCD2-1 are noncooperative whereas those with βCD2-2 and *c*-βCD2 are cooperative. The analysis of data will be also described in the following subsection.

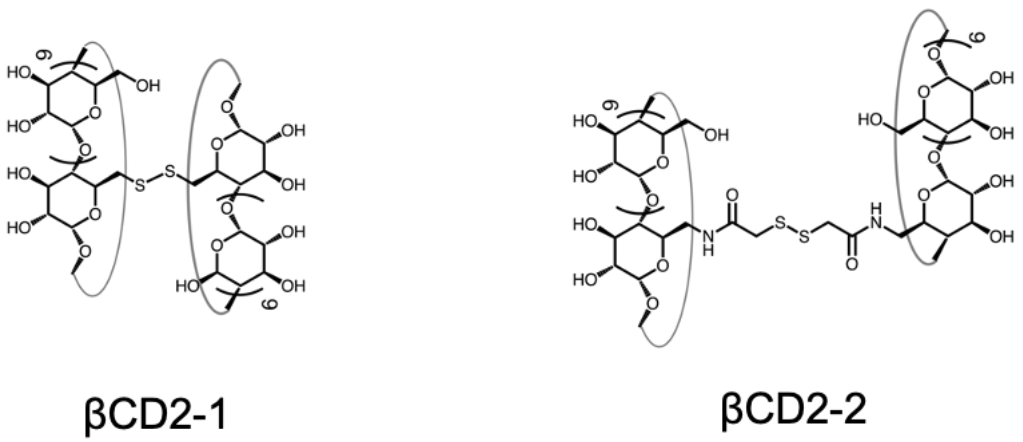

Figure 4-5. Chemical structures of βCD2-1 and βCD2-2.

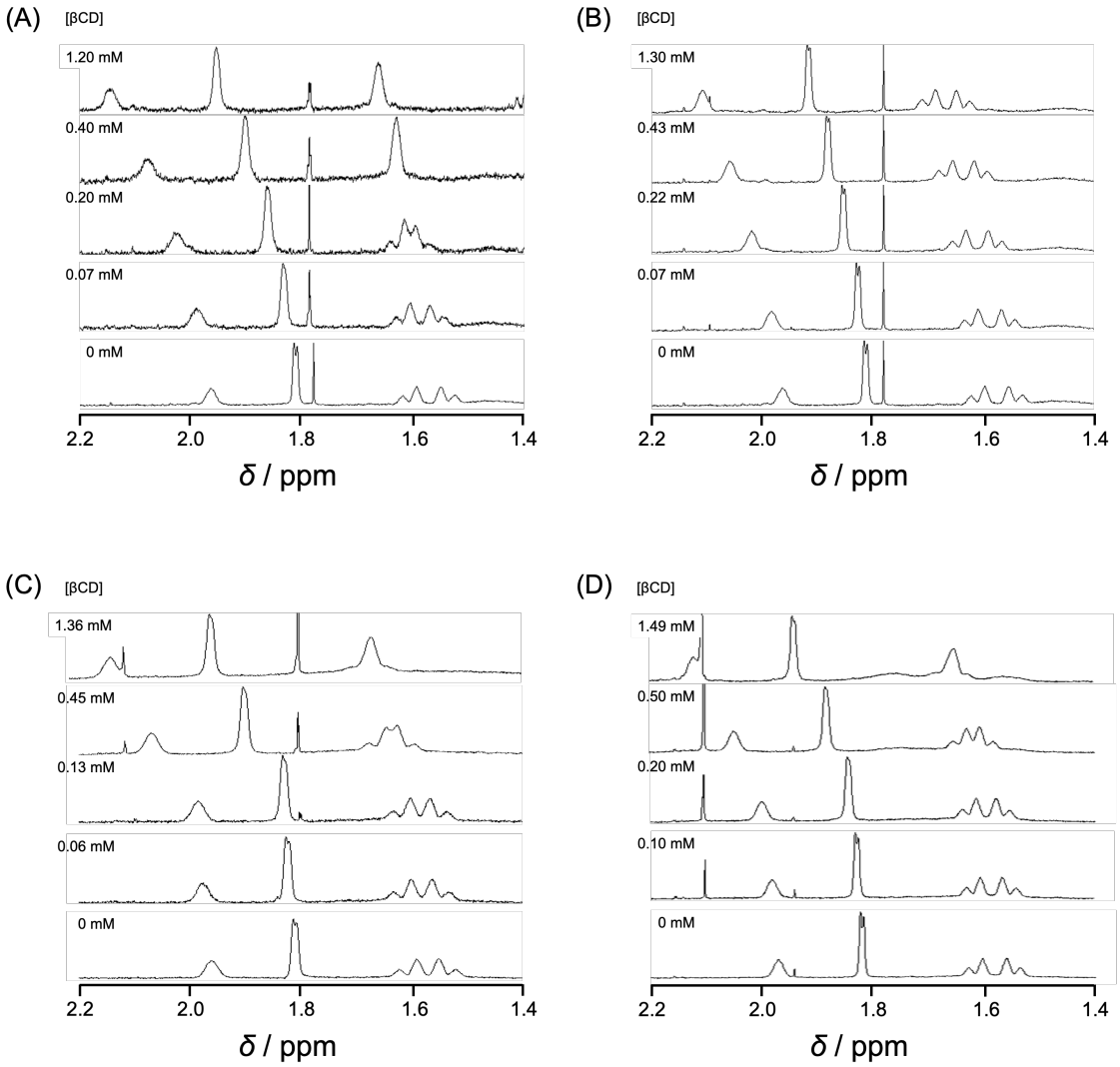

Figure 4-6. ^{1}H NMR spectra for *c*-Ad2 at different concentrations of βCD (A), βCD2-1 (B), βCD2-2 (C), and *c*-βCD2 (D).

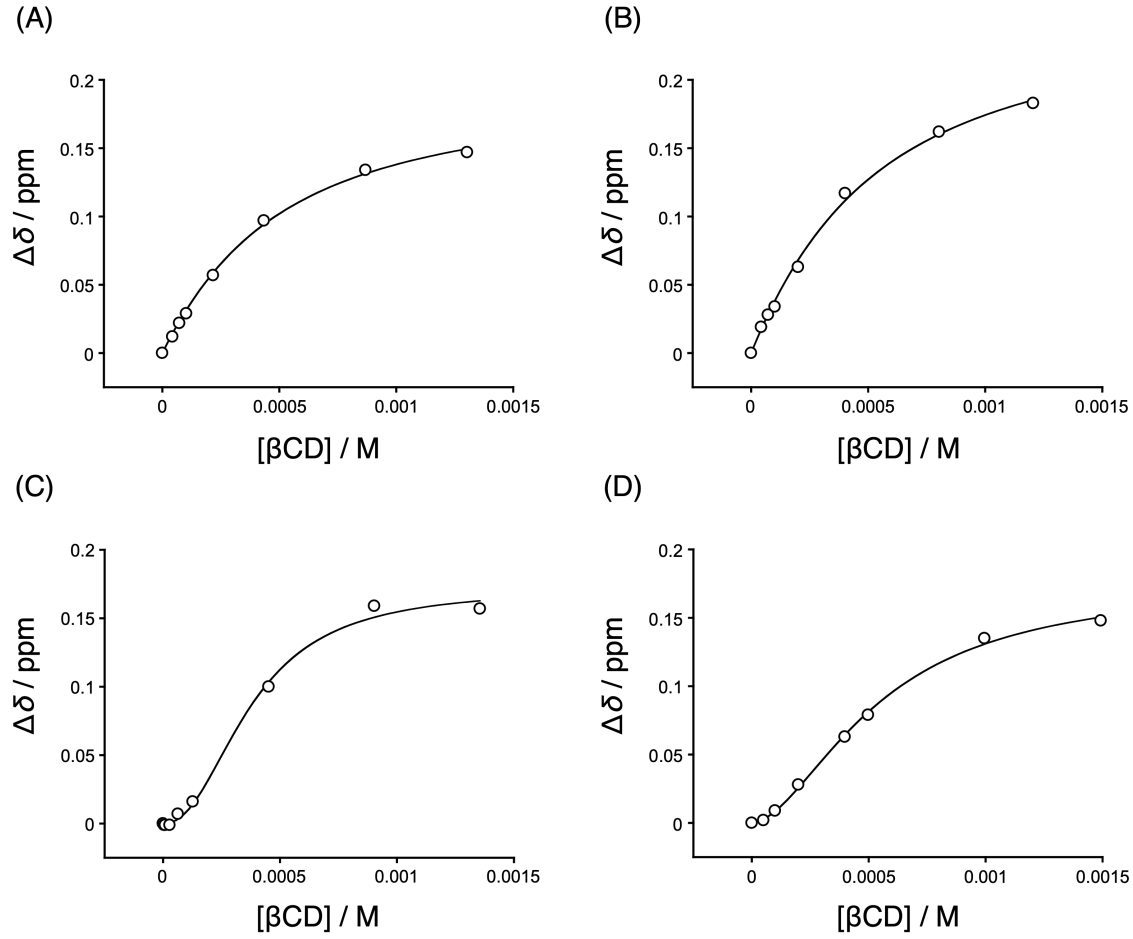

Figure 4-7. Plots of Δδ against βCD concentration for solutions of *c*-Ad2 with βCD (A), βCD2-1 (B), βCD2-2 (C), and *c*-βCD2 (D) with a best-fit curve using eqs 4-16 (A and B) and 4-17 (C and D).

4-4. Discussion

Interaction of p(AANa/Np*x*) with βCD and *c*-βCD2. *(a) The Formation of One-to-One Complexes between Np and βCD Moieties.* The equilibrium equation for the formation of one-to-one complexes (Np•βCD) is as follows:

$$\text{Np} + \beta\text{CD} \underset{}{\overset{K_1}{\rightleftharpoons}} \text{Np}\bullet\beta\text{CD}$$

Given that [Np], [βCD], and [Np•βCD] are the concentrations of Np, βCD, and Np•βCD, respectively, the association constant K_1 is defined by

$$K_1 = \frac{[\text{Np}\bullet\beta\text{CD}]}{[\text{Np}][\beta\text{CD}]} \tag{4-1}$$

From the conservation of mass,

$$[\text{Np}]_0 = [\text{Np}] + [\text{Np} \bullet \beta\text{CD}] \tag{4-2}$$

$$[\text{Np} \bullet \beta\text{CD}] = [\text{Np}]_0 - [\text{Np}] \tag{4-3}$$

where $[\text{Np}]_0$ is the total concentration of Np. To simplify this model, βCD is assumed to be greatly in excess of Np, and $[\beta\text{CD}] = [\beta\text{CD}]_0$.

From eqs 4-1 and 4-3,

$$K_1 = \frac{[\text{Np}]_0 - [\text{Np}]}{[\text{Np}][\beta\text{CD}]} \tag{4-4}$$

$$[\text{Np}] = \frac{[\text{Np}]_0}{1 + K_1[\beta\text{CD}]} \tag{4-5}$$

Given that I_0 and I are the fluorescence intensities in the absence and presence of βCD, respectively, the ratio I/I_0 is written as

$$I/I_0 = \frac{k_0[\text{Np}] + k_1[\text{Np}\bullet\beta\text{CD}]}{k_0[\text{Np}]_0} \tag{4-6}$$

where k_0 and k_1 are the ratios of fluorescence quantum yields to the molar absorption coefficient of Np and Np•βCD, respectively. k_0 of Np is assumed to be unchanged in the presence and absence of βCD. From eqs 4-3, 4-5, and 4-6,

$$I/I_0 = \frac{1+(k_1/k_0)K_1[\beta\mathrm{CD}]_0}{1+K_1[\beta\mathrm{CD}]_0} \quad (4\text{-}7)$$

In Figures 4-3A and 4-3B, when the K_1 values and k_1/k_0 are chosen appropriately, the calculated I/I_0 using eq 4-7 fairly agree with the experimental values. From these fittings, the association constants for p(AANa/Np6) and p(AANa/Np15) with βCD were estimated to be 6.0×10^2 and 1.5×10^3 M^{-1}, respectively. The K_1 for p(AANa/Np15) with βCD is larger than for p(AANa/Np6) with βCD likely because of lower solubility of p(AANa/Np15) due to higher content of Np moieties.

(b) The Formation of Higher-Order Complexes between Np and βCD Moieties. On the other hand, in the cases of *c*-βCD2, the calculated I/I_0 did not agree with the experimental values. Thus, the data for *c*-βCD2 were analyzed using a model proposed for the formation of two-to-two complexes. The equilibrium equations for the formation of two-to-two complexes formation are as follows:

$$\mathrm{Np^2} + \beta\mathrm{CD} \overset{K_1}{\rightleftharpoons} \mathrm{Np^2{\bullet}\beta CD}$$

$$\mathrm{Np^2{\bullet}\beta CD} + \beta\mathrm{CD} \overset{K_2}{\rightleftharpoons} \mathrm{Np^2{\bullet}\beta CD_2}$$

where Np^2, βCD, Np^2•βCD, and Np^2•βCD_2 are Np dimer, a βCD residue, the two-to-one complex, and the two-to-two complex, respectively. Given that [Np^2], [βCD], [Np^2•βCD], and [Np^2•βCD_2] are the concentrations of Np^2, βCD, Np^2•βCD, and Np^2•βCD_2,

respectively, the association constants K_1 and K_2 are defined by

$$K_1 = \frac{[\mathrm{Np^2 \bullet \beta CD}]}{[\mathrm{Np^2}][\beta\mathrm{CD}]} \tag{4-8}$$

$$K_2 = \frac{[\mathrm{Np^2 \bullet \beta CD_2}]}{[\mathrm{Np^2 \bullet \beta CD}][\beta\mathrm{CD}]} \tag{4-9}$$

From the conservation of mass,

$$[\mathrm{Np^2}]_0 = [\mathrm{Np^2}] + [\mathrm{Np^2 \bullet \beta CD}] + [\mathrm{Np^2 \bullet \beta CD_2}] \tag{4-10}$$

$$[\beta\mathrm{CD}]_0 = [\beta\mathrm{CD}] + [\mathrm{Np^2 \bullet \beta CD}] + 2[\mathrm{Np^2 \bullet \beta CD_2}] \tag{4-11}$$

From eqs 4-8, 4-9, and 4-10,

$$[\mathrm{Np^2}] = \frac{[\mathrm{Np^2}]_0}{1+K_1[\beta\mathrm{CD}](1+K_2[\beta\mathrm{CD}])} \tag{4-12}$$

$$[\mathrm{Np^2 \bullet \beta CD}] = \frac{K_1[\mathrm{Np^2}]_0[\beta\mathrm{CD}]}{1+K_1[\beta\mathrm{CD}](1+K_2[\beta\mathrm{CD}])} \tag{4-13}$$

$$[\mathrm{Np^2 \bullet \beta CD_2}] = \frac{K_1K_2[\mathrm{Np^2}]_0[\beta\mathrm{CD}]^2}{1+K_1[\beta\mathrm{CD}](1+K_2[\beta\mathrm{CD}])} \tag{4-14}$$

Thus, if the values for $[Np^2]_0$, [βCD], K_1, and K_2 are given, all the concentrations of Np species, i.e., $[Np^2]$, $[Np^2\bullet\beta CD]$, and $[Np^2\bullet\beta CD_2]$, can be calculated with eqs 4-12, 4-13, and 4-14. Since $[\beta CD]_0$ can be also calculated with eq 4-11, $[Np^2]$, $[Np^2\bullet\beta CD]$, and $[Np^2\bullet\beta CD_2]$ can be plotted against $[\beta CD]_0$. Given that I_0 and I are the fluorescence intensities in the absence and presence of βCD, respectively, the ratio I/I_0 is written as

$$I/I_0 = \frac{k_0[\mathrm{Np^2}]+k_1[\mathrm{Np^2 \bullet \beta CD}]+k_2[\mathrm{Np^2 \bullet \beta CD_2}]}{k_0[\mathrm{Np^2}]_0} \tag{4-15}$$

where k_0, k_1, and k_2 are the ratio of fluorescence quantum yields to the molar absorption coefficient of Np^2, $Np^2\bullet\beta CD$, and $Np^2\bullet\beta CD_2$, respectively. k_0 of Np^2 is assumed to be

unchanged in the presence and absence of βCD.

In Figures 4-3C and 4-3D, when the K_1, K_2, k_1/k_0, and k_2/k_0 values are chosen appropriately, the I/I_0 values calculated using eq 4-15 fairly agree with the experimental values. From these fittings, the association constants K_1 and K_2 for p(AANa/Np6) with *c*-βCD2 were estimated to be 2.0×10^4 and 7.5×10^2 M^{-1}, respectively. K_1 and K_2 values for p(AANa/Np15) and *c*-βCD2 were estimated to be 2.5×10^4 and 6.0×10^2 M^{-1}, respectively. It should be noted here that K_2 is smaller than K_1 in both the cases of p(AANa/Np6) and p(AANa/Np15), indicative of negative cooperativity.

Here the author discusses why the interactions of p(AANa/Np6) and p(AANa/Np15) with *c*-βCD2 show negative cooperativity. Assuming that Np moieties are statistically introduced onto p(AANa/Np6) and p(AANa/Np15), the average number of monomer units between two Np moieties are 15.7 and 5.7 for p(AANa/Np6) and p(AANa/Np15), respectively. Figure 4-8 shows typical three-dimensional structures of parts of p(AANa/Np6) and p(AANa/Np15), and *c*-βCD2, optimized by molecular mechanics on a Chem3D software. The intervals of Np moieties of p(AANa/Np6) and p(AANa/Np15) estimated using nitrogen atoms in amide bonds are ca. 40 and 19 Å, respectively. On the other hand, the distance between the centers of βCD moieties in *c*-βCD2 is ca. 35 Å. The interval of Np moieties in p(AANa/Np6) is larger than that of the

βCD moieties in *c*-βCD2, while the interval of Np moieties in p(AANa/Np15) is smaller than that of the βCD moieties in *c*-βCD2. It is thus likely that the mismatch of intervals of Np and βCD moieties is responsible for the negative cooperativity observed in the interactions of p(AANa/Np6) and p(AANa/Np15) with *c*-βCD2 (Figure 4-9).

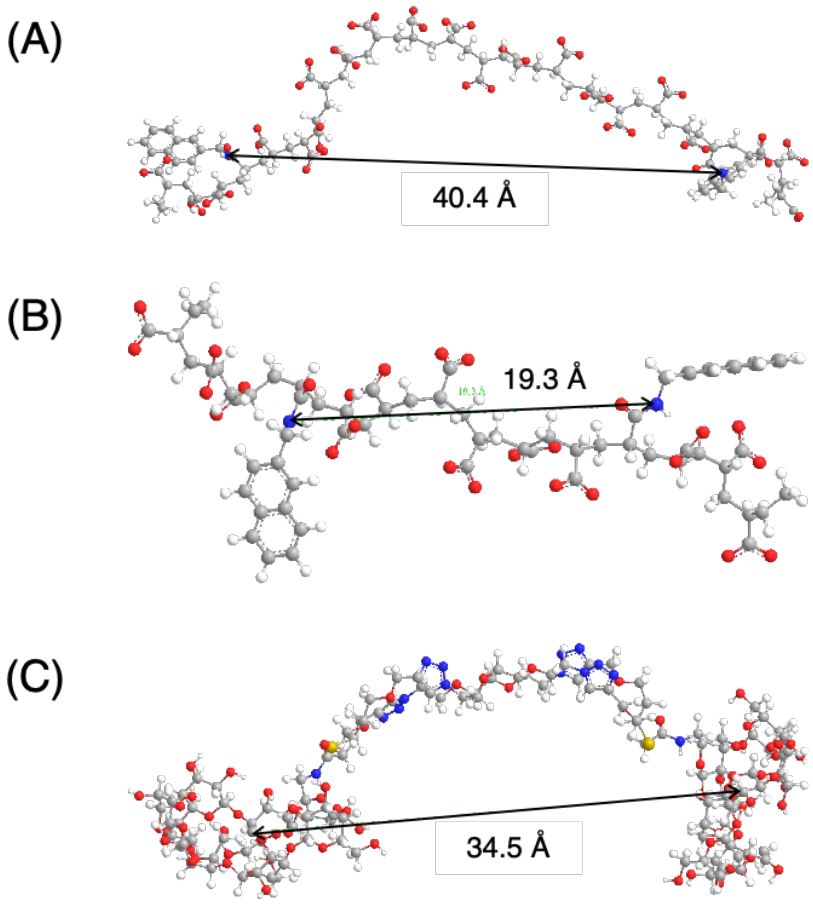

Figure 4-8. Typical 3D structures of parts of p(AANa/Np6) (A) and p(AANa/Np15) (B), and *c*-βCD2 (C).

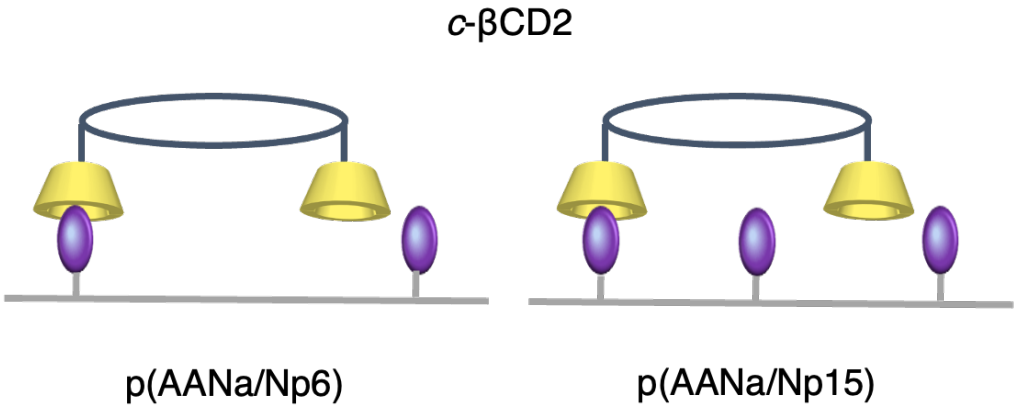

Figure 4-9. Conceptual illustrations of the interactions of p(AANa/Np6) and p(AANa/Np15) with *c*-βCD2.

Interaction of *c*-Ad2 with several hosts. *(a) The Formation of One-to-One Complexes between Ad and βCD Moieties.* The interaction between poly(acrylic acid) bearing Np moieties and *c*-βCD2 showed negative cooperativity due to mismatch of intervals of interacting residues. Therefore, the interaction of complementary guest dimer bearing Ad moieties (*c*-Ad2) and several hosts containing *c*-βCD2 was investigated using NMR techniques. Assuming one-to-one complex formation, the apparent values of association constant (K_a) were estimated by fitting the data with

$$\Delta\delta = \frac{\Delta\delta_{max}}{2K_a[\mathrm{Ad}]} \times \left[1 + K_a[\beta\mathrm{CD}] + K_a[\mathrm{Ad}] - \{(1 + K_a[\beta\mathrm{CD}] + K_a[\mathrm{Ad}])^2 - 4K_a^2[\beta\mathrm{CD}][\mathrm{Ad}]\}^{\frac{1}{2}}\right] \quad (4\text{-}16)$$

where $\Delta\delta_{max}$ is the saturated values of $\Delta\delta$, and [Ad] is the concentration of Ad moiety.

In the cases of βCD and βCD2-1, when the K_a values are chosen appropriately, the calculated $\Delta\delta$ using eq 4-16 agree with the experimental values (Figures 4-7A and 4-7B).

(b) The Cooperative Interaction. On the other hand, in the cases of βCD2-2 and *c*-βCD2, the calculated $\Delta\delta$ based on the one-to-one complexation did not agree with the experimental values, because the date obeyed a sigmoidal curve (Figures 4-7C and 4-7D). Thus, the data for βCD2-2 and *c*-βCD2 were analyzed using the Hill model, i.e., one of the typical models for cooperative interaction:

$$\Delta\delta = \frac{[\beta\mathrm{CD}]^n}{(\frac{1}{K_a})^n + [\beta\mathrm{CD}]^n}\Delta\delta_{\max} \tag{4-17}$$

where n is the Hill coefficient. As can be seen in Figures 4-7C and 4-7D, when n, $\Delta\delta_{\max}$, and association constants were chosen appropriately, the calculated values of $\Delta\delta$ agree with the experimental values.

The estimated K_a and n are summarized in Table 1. The interactions of *c*-Ad2 with βCD and with βCD2-1 were explained by a one-to-one complex formation model. The K_a values for the *c*-Ad2/βCD and *c*-Ad2/βCD2-1 were almost the same, indicating that βCD2-1 behaves as a monofunctional host. The K_a for *c*-Ad2 with βCD2-1 is approximately twice that for *c*-Ad2 with βCD when βCD concentration is converted to βCD2-1 concentration. This may be because the local concentration of βCD increased in the case of βCD2-1. On the other hand, the interactions of *c*-Ad2 with βCD2-2 and with

c-CD2 were explained by the Hill model with $n \sim 2$, indicative of positive cooperativity.

Table 4-1. Association Constants (K_a) and Hill Coefficients (n) for the Interactions of *c*-Ad2 with Host Molecules

Host	K_a / 10^{-3} M^{-1}	n
βCD[a]	2.68 ± 0.26	–
βCD2-1[a]	2.44 ± 0.30	–
βCD2-2[b]	2.66 ± 0.19	2.2 ± 0.3
c-βCD2[b]	1.84 ± 0.13	1.8 ± 0.1

a. Estimated using a model assuming 1:1 complex formation. *b*. Estimated using Hill equation.

Here the author discusses why the interactions of *c*-Ad2 with βCD2-2 and *c*-βCD2 show positive cooperativity. Figure 4-10 shows typical three-dimensional structures of *c*-Ad2, βCD2-1, and βCD2-2, optimized by molecular mechanics on a Chem3D software. The interval of Ad moieties in *c*-Ad2 estimated using sulfur atoms is ca. 23 Å. The distances between the centers of βCD moieties in βCD2-1 and βCD2-2 are ca. 14 and 20 Å, respectively. The interval of Ad moieties is larger than that of βCD

moieties in βCD2-1, while the interval of Ad moieties is close to that of βCD moieties in βCD2-2. Since *c*-βCD2 is complementary to *c*-Ad2, the intervals of the interacting residues are the same. Therefore, the interval matching of Ad and βCD moieties is responsible for the positive cooperativity observed in the interactions of *c*-Ad2 with βCD2-2 and *c*-βCD2 (Figure 4-11).

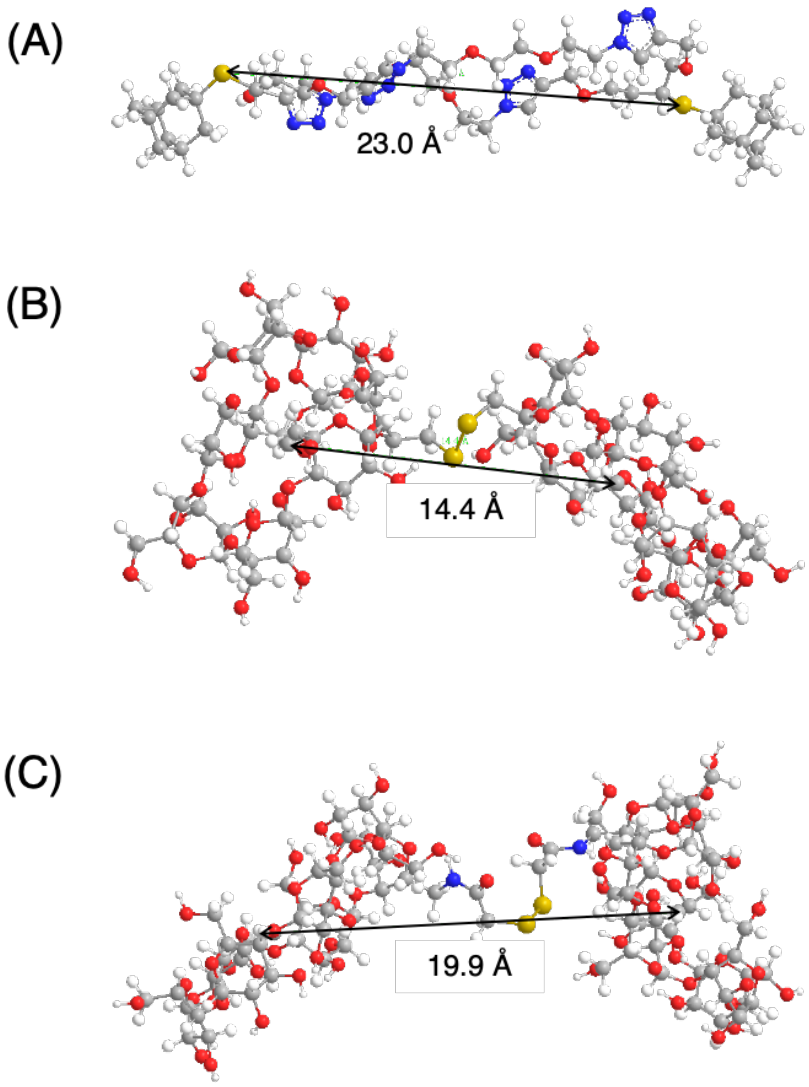

Figure 4-10. Typical 3D structures of *c*-Ad2 (A), βCD2-1 (B), and βCD2-2 (C).

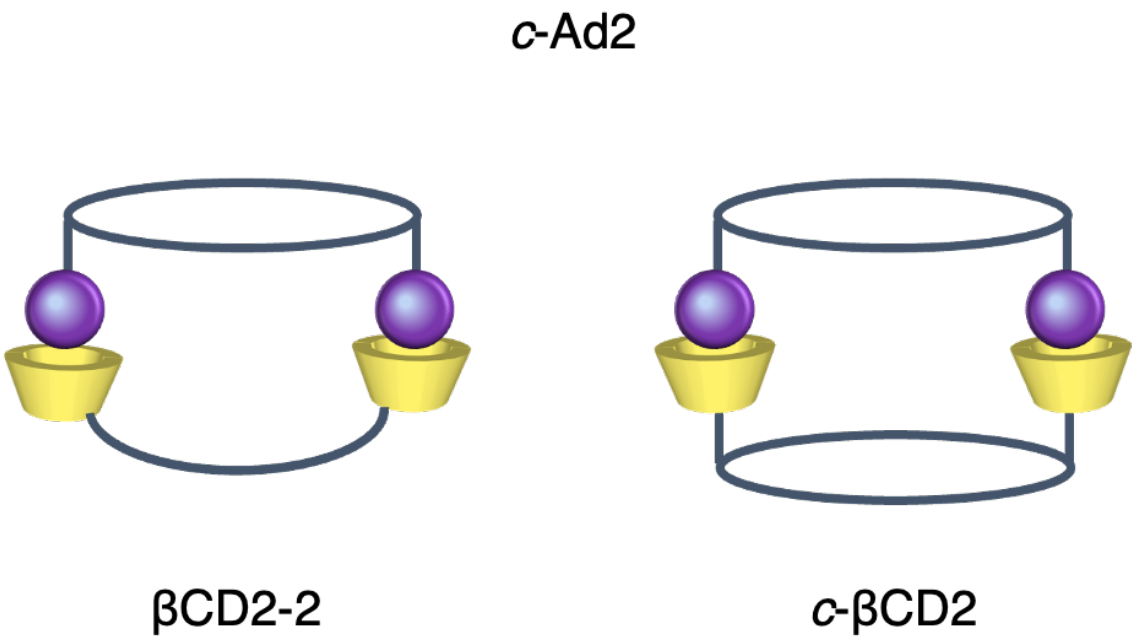

Figure 4-11. Conceptual illustrations of the interactions of *c*-Ad2 with βCD2-2 and *c*-βCD2.

To obtain information about the structure of complexes, the *c*-Ad2/βCD2-2 and *c*-Ad2/*c*-CD2 mixtures were characterized by PGSE NMR using D_2O as a solvent. Figure 4-12A indicates the signals due to *c*-Ad2 in the diffusion coefficient (*D*) region of (4–9) × 10^{-10} m^2 s^{-1}. There are the signals due to *c*-Ad2 in the presence of βCD2-2 and *c*-βCD2 in the *D* regions of (3–6) × 10^{-10} and (2–5) × 10^{-10} m^2 s^{-1}, as can be seen in Figures 4-12B and 4-12C, respectively. Using the signal attributed to the methine proton in Ad moiety at ca. 2 ppm, the *D* values for *c*-Ad2 in the absence and presence of βCD2-2 and *c*-βCD2 were evaluated to be 8.8 × 10^{-10}, 3.5 × 10^{-10}, and 3.8 × 10^{-10} m^2 s^{-1}, respectively.

On the basis of these *D* values, the hydrodynamic radii (R_H) were calculated to be ca. 2.3, 5.8, and 5.3 nm, respectively, using the Einstein–Stokes equation. These data indicate that the *c*-Ad2/βCD2-2 and *c*-Ad2/*c*-βCD2 mixtures formed closed complexes (Figure 4-11), not supramolecular polymers.

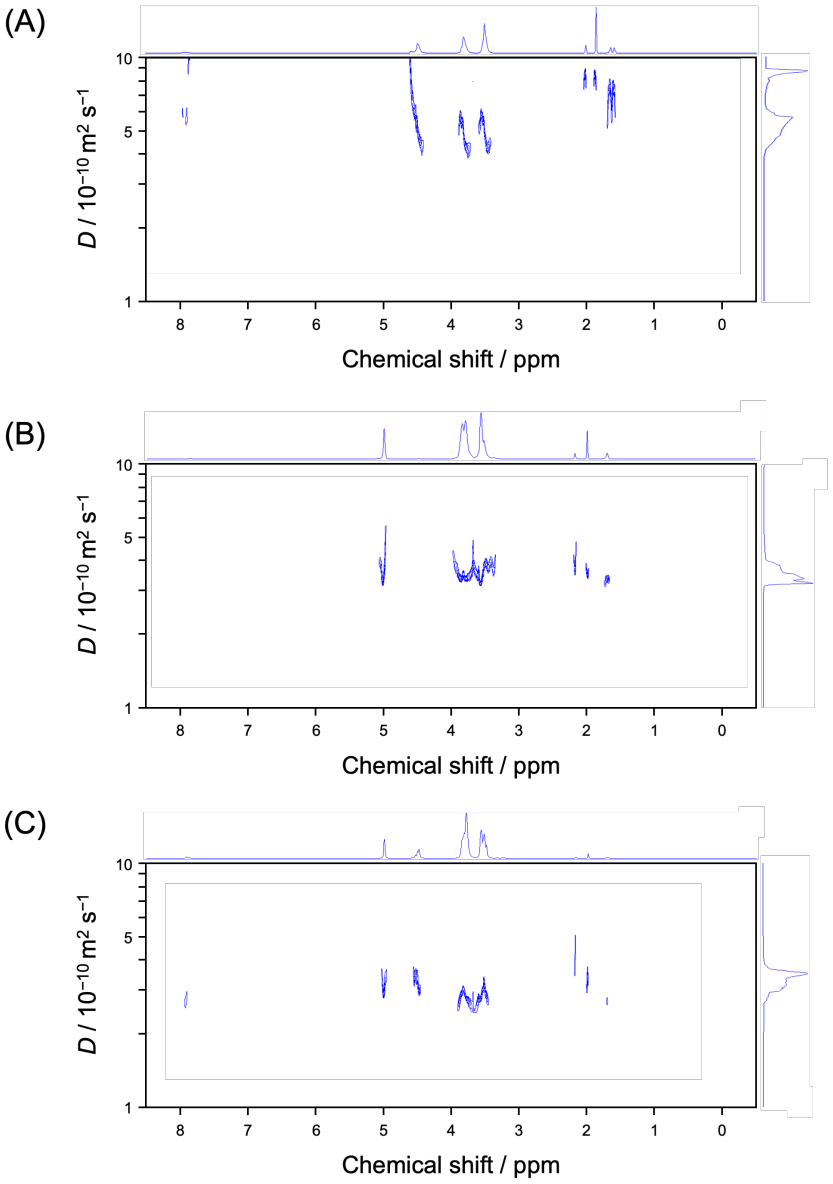

Figure 4-12. DOSY for *c*-Ad2 without βCD (A), and with βCD2-2 (B) and *c*-βCD2 (C).

4-5. Conclusions

In this chapter, the author first focused on the polymer/dimer interaction systems. The interactions of polyacrylic acid (p(AANa/Np*x*)) bearing Np residues of different continents with βCD and *c*-βCD2 were investigated by fluorescence measurements. The interactions of p(AANa/Np*x*) with βCD were explained by a one-to-one complex formation model. The K_1 values for p(AANa/Np6) and p(AANa/Np15) with βCD were estimated to be 3500 and 6000 M^{-1}, respectively. On the other hand, the interactions of p(AANa/Np*x*) with *c*-βCD2 were explained by a model for the formation of higher-order complexes. In the case of p(AANa/Np6), the K_1 and K_2 values were estimated to be 2000 and 150 M^{-1}, respectively. The K_1 and K_2 values for p(AANa/Np15) with *c*-βCD2 were estimated to be 25000 and 70 M^{-1}. In both cases of p(AANa/Np6) and p(AANa/Np15), K_2 was smaller than K_1, indicative of negative cooperativity. Based on the comparison of three-dimensional models of the partial structure of p(AANa/Np*x*) and the structure of *c*-βCD2, it is likely that the mismatched intervals are responsible for the negative cooperativity. The author also focused on the interaction of *c*-Ad2. The interactions of *c*-Ad2 with βCD, βCD dimers linked by disulfide bonds (βCD2-1 and βCD2-2), and the cyclic host dimer (*c*-βCD2) were investigated by ^{1}H NMR. The interactions of *c*-Ad2 with βCD and βCD2-1 can be explained by a model based on one-to-one inclusion complex

formation. On the other hand, the interactions of *c*-Ad2 with βCD2-2 and with *c*-βCD2 were explained by the Hill model with $n \sim 2$, indicative of positive cooperativity. Based on the comparison of three-dimensional models of the structure of *c*-Ad2, βCD2-2, and *c*-βCD2, it is likely that the matched intervals are responsible for the positive cooperativity. The *c*-Ad2/βCD2-2 and *c*-Ad2/*c*-βCD2 mixtures were characterized by PGSE NMR. The R_H values were calculated by the Einstein-Stokes equation to be ca. 5.7 and 5.3 nm for the *c*-Ad2/βCD2-2 and *c*-Ad2/*c*-βCD2 complexes, respectively. Whereas R_H for *c*-Ad2 was ca. 2.3 nm. These data indicate that the *c*-Ad2/βCD2-2 and *c*-Ad2/*c*-βCD2 mixtures formed closed complexes, not supramolecular polymers.

4-6. References

(1) Voet, D.; Voet, J. G. Biochemistry; 4th ed.; Wiley & Sons: New York, 2010.

(2) Gillies, E. R.; Fréchet, J. M. J. *Drug Discovery Today.* **2005**, *10*, 35–43.

(3) Hagg, R.; Kratz, F. *Angew. Chem. Int. Ed.* **2006**, *45*, 1198–1215.

(4) Fasting, C.; Schalley, C. A.; Weber, M.; Seitz, O.; Hecht, S.; Koksch, B.; Dernedde, J.; Graf, C.; Knapp, E.-W.; Haag, R. *Angew. Chem., Int. Ed.* **2012,** *51,* 10472–10498.

(5) Harada, A.; Takashima, Y.; Nakahata, M. *Acc. Chem. Res.* **2014**, *47*, 2128−2140.

(6) Hu, J.; Liu, S. *Acc. Chem. Res.* **2014**, *47*, 2084−2095.

(7) Huo, Y.; He, Z.; Wang, C.; Zhang, L.; Xuan, Q.; Wei, S.; Wang, Y.; Pan, D.; Dong, B.; Wei, R.; Naik, N.; Guo, Z. *Chem. Commun.* **2021**, 57, 1413–1429.

(8) Heinzmann, C.; Weder, C.; de Espinosa, L. M. *Chem. Soc. Rev.* **2016**, *45*, 342–358.

(9) Lu, W.; Le, X.; Zhang, J.; Huang, Y.; Chen, T. *Chem. Soc. Rev.* **2017**, *46*, 1284–1294.

(10) Danyu Xia, D.; Wang, P.; Ji, X.; Khashab, N. M.; Sessler, J. L.; Huang, F. *Chem. Rev.* **2020**, *120*, 6070–6123.

(11) Agasti, S. S.; Tassa, M. L. C.; Chung, H. J. C.; Shaw, S. Y.; Lee, H.; Weissleder, R. *Angew. Chem. Int. Ed.* **2012**, 51, 450–454.

(12) Yamamura, H.; Yamada, S.; Kohno, K.; Okuda, N.; Araki, S.; Kobayashi, K.; Katakai, R.; Kano, K.; Kawai, M. *J. Chem. Soc., Perkin Trans.* **1999**, *1*, 2943–2948.

(13) Stejskal, E. O.; Tanner, J. E. *J. Chem. Phys.* **1965**, *42*, 288–292.

(14) Tanner, J. E.; Stejskal, E. O. *J. Chem. Phys.* **1968**, *49*, 1768–1777.

(15) Stilbs, P. *Prog. Nucl. Magn. Reson. Spectrosc.* **1987**, *19*, 1–45.

(16) Morris, K. F.; Stilbs, P.; Johnson, C. S. *Anal. Chem.* **1994**, *66*, 211–215.

(17) Huo, R.; Wehrens, R.; Van Duynhoven, J.; Buydens, L. M. C. *Anal. Chim. Acta* **2003**, *490*, 231–251.

(18) Lligadas, G.; Percec, V. J. Polym. *Sci., Part A: Polym. Chem.* **2007**, *45*, 4684−4695.

(19) Ma, Q.; Wooley, K. L. J. *Polym. Sci., Part A: Polym. Chem.* **2000**, *38*, 4805−4820.

(20) Tomatsu, I.; Hashidzume A.; Harada, A. *Macromol. Rapid Commun.* **2005**, *26*, 825–829.

Chapter 5

Conclusions

In this thesis, the author synthesized interval-controlled polymers and oligomers using monodisperse oligo(ethylene glycol)s (MD-OEGs) by click chemistry. The specific properties of the polymers and oligomers based on controlled intervals were investigated.

In Chapter 2, the author synthesized network polymers by thiol–yne reaction of dithiol (DT-EG*n*) and dialkyne (DY-EG*n*) formed from MD-OEGs of different degrees of polymerization *n* to investigate the effect of *n* on the mechanical properties. The authors first monitored the thiol–yne reaction of DT-EG*n* and DY-EG*n* by IR measurements of thin films. IR spectra indicated that the thiol–yne reactions for $n = 2$, 3, and 4 were completed within 60 s. Since the efficient progress of the thiol–yne reaction was observed, the authors prepared disk-shape samples for compression tests to investigate mechanical properties. From the stress-strain curves obtained from the compression tests, Young's moduli *E* for the samples were estimated. The *E* decreased from 18.2 to 12.6 MPa with *n* increased from 2 to 4 due to the decrease in crosslinking density with increasing *n*.

In Chapter 3, the author synthesized cyclic dimers bearing Ad and βCD moieties

as interacting residues. The uniform cyclic dimer (*c*-ene2) was synthesized by stepwise CuAAC of a diazide formed from triethylene glycol and a dialkyne possessing an internal alkene. The author obtained the cyclic guest dimer bearing Ad moieties (*c*-Ad2) by thiol–ene reaction. The cyclic host dimer bearing βCD moieties (*c*-βCD2) by a combination of thiol–ene reaction and amide-coupling. The dimers were characterized by NMR and MS.

In Chapter 4, the authors investigated the interaction of the cyclic dimers synthesized in Chapter 3. The interaction of *c*-βCD2 with poly(acrylic acid)s bearing naphthyl moieties (p(AANa/Np*x*), where *x* is the mol% content of the Np moieties) was investigated by fluorescence measurements. The interaction of *c*-βCD2 with p(AANa/Np*x*) showed negative cooperativity due to the mismatch of intervals between naphthyl and βCD moieties. The interaction of *c*-Ad2 complimentary to *c*-βCD2 was investigated by NMR techniques. The interaction of *c*-Ad2 with *c*-βCD2 and with the βCD dimer linked by a disulfide linker of appropriate length showed cooperativity presumably because of the matched intervals between Ad and βCD moieties.

In conclusion, the author successfully synthesized interval-controlled polymers and oligomers by a combination of MD-OEGs and click chemistry. The polymers and oligomers exhibited properties based on controlled intervals. The author believes that this work presented here will contribute significantly to motivating and facilitating synthesis

of interval-controlled polymers and oligomers with a variety of functions.

List of Publications

(1) Mechanical Properties of Network Polymers Formed from Monodisperse Oligo(ethylene glycol)s of Different Molecular Weights through Thiol–Yne Reaction

Ishitsuka, K.; Pagaduan, J. N. M.; Kamon, Y.; Hashidzume, A. *Mater. Today Commun.* **2020**, *22*, 100689. (Chapter 2)

(2) Synthesis of Interval-Controlled Cyclic Dimers by Click Chemistry and Their Interaction

Ishitsuka, K.; Nakahata. M.; Kamon, Y.; Hashidzume, A. to be published (Chapter 3 and 4)